Journal of Structural Geology xxx (2014) 1–18

Contents lists available at ScienceDirect

Journal of Structural Geology

journal homepage: www.elsevier.com/locate/jsg

Microfractures: A review

Mark H. Anders [a,*], Stephen E. Laubach [b], Christopher H. Scholz [a]

[a] Department of Earth and Environmental Sciences, Lamont-Doherty Earth Observatory of Columbia University, Palisades, NY 10964, USA
[b] Bureau of Economic Geology, The University of Texas at Austin, Austin, TX 78713, USA

Keywords:
Fault
Fluid-inclusion planes
Fracture
Microfractures
Paleostress
Scaling

A B S T R A C T

Microfractures are small, high-aspect-ratio cracks in rock that result from application of differential stresses. Although the term has been used to refer to larger features in the petroleum engineering and geophysics literature, in geologic parlance the term refers to fractures visible only under magnification, having lengths of millimeters or less and widths generally less than 0.1 mm. Nevertheless, populations of these structures typically encompass a wide size range and in some cases they form the small-size fraction of fracture arrays that include much larger factures. In geologic settings, microfractures commonly form as Mode I (opening) fractures where the minimum principal stress exceeds the elastic tensile strength creating a narrow opening displacement; in isotropic rocks such fractures mark the plane perpendicular to the least compressive principal stress during fracture growth. These planar or curviplanar openings provide an opportunity for fluids and/or gases to enter the created cavity. Cement deposits or crack closure may trap fluids or gases, leaving mineral precipitates and a track of enclosed fluids and gases. In transmitted light these precipitates frequently manifest as fluid-inclusion planes (FIPs). Cathodoluminescence (CL) images show that many are cement-filled microveins. Microfractures can be used to assess the paleostress history or fluid movement history of a rock body. Also, because sudden opening produces acoustic emissions, microfractures created in the laboratory can be used to assess the rock-failure process. Here we review recent discoveries made using microfractures, including fracture patterns, strain, fracture growth and size-scaling, evolution of stresses around propagating faults (process zones), far-field tectonic stresses, and insights into the state of stress leading to earthquakes.

1. Introduction

Microfractures are lens-shaped or tabular opening-mode (Mode I) high-aspect-ratio fractures with dimensions so small that they usually require microscopy to detect. Microfractures can govern physical rock properties such as strength, elastic wave velocities, and permeability. As we describe below, microfractures are useful in providing evidence for temperature of fracturing, fluid conditions, and timing. In sedimentary basins they provide key evidence of the processes of compaction, consolidation, and the patterns of fluid flow. Experimentally produced microfractures (microcracks) provide insight to the process of rock failure and the causes of seismic anisotropy. Studies of microfracture orientations provide critical information on the growth and development of fault zones, the evolution of regional stress fields, and the earthquake cycle.

A microfracture review by Kranz (1983) summarized a decade of intense work, primarily in the laboratory, that revealed how microfractures govern physical rock properties such as strength, elastic wave velocities, and permeability. But major reviews of (macro) fracture growth and attributes from that time (e.g., Hancock, 1985; Pollard and Aydin, 1988) largely or entirely ignore microfractures. Although experimental (and theoretical) work emphasized the role of microfractures (for example, as nucleation sites for larger fractures), microfractures were missing from mainstream accounts of fracture patterns, despite — as we will see — the existence of petrographic tools capable of detecting microfractures and an older (separate) literature that documented the coexistence of microfracture and macrofracture populations. In retrospect, this circumstance may have resulted from the almost complete lack of microfractures associated with large, barren opening-mode fractures formed near the Earth's surface (i.e., joints), the principal focus of macrofracture studies from the 1960s to 1980s. But there is no evidence that such microfractures were sought; and their absence, which is probably significant, was not remarked. This lack of scrutiny suggests a gap in theories of fracture

* Corresponding author.
E-mail addresses: manders@ldeo.columbia.edu (M.H. Anders), steve.laubach@beg.utexas.edu (S.E. Laubach).

http://dx.doi.org/10.1016/j.jsg.2014.05.011

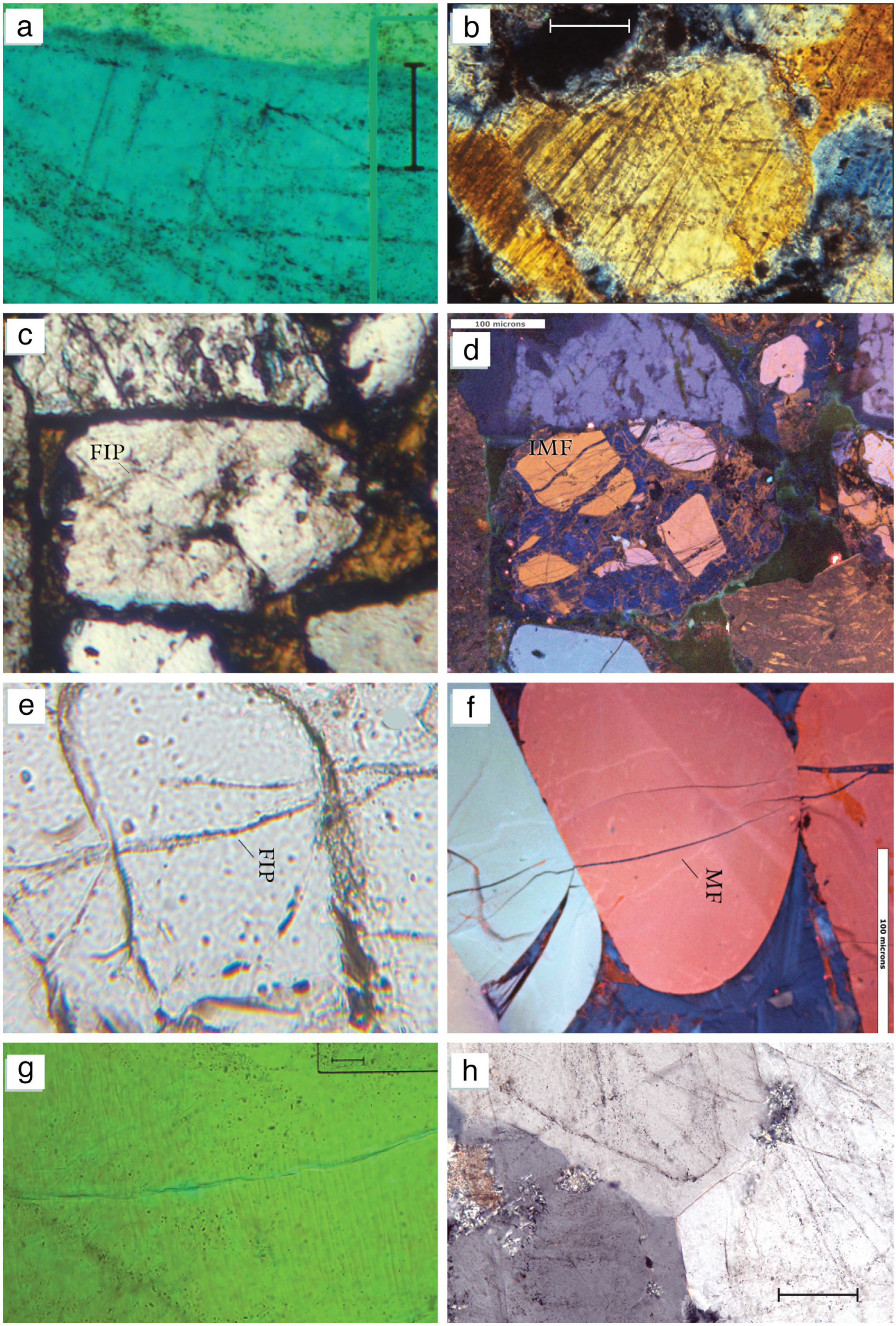

Fig. 1. (a) Transmitted light (TL) image of microfractures in a Tertiary granite, Mineral Mountains, Utah. Note the small isolated particles, which define the plane of the microfracture (FIP). Scale bar 100 μm. (b) TL image of microfractures (FIP) in the Lyon Sandstone, near Boulder, Colorado. The microfractures are intragranular and demonstrate a strong preferred orientation. From Anders and Wiltschko (1994). Scale bar 100 μm. (c) Inherited fractures in Cretaceous Frontier Formation sandstone sand grain under plane-polarized transmitted light, showing inherited fluid-inclusion planes (FIP). (d).Color SEM-CL of same area as (c), showing inherited microfractures, IMF (microveins) truncated at grain margin. Note the

growth. By the late 1980s a community of research on natural microfractures existed, but these workers were already separate from the macrofractures/joints community.

Our aim here is to provide the historical context of microfracture research that can help guide future work and to provide commentary and examples that will direct the hitherto disparate communities studying microfractures to problems of common interest. We review recent discoveries made using microfractures, including fracture patterns, strain, fracture growth and size-scaling, evolution of stresses around propagating faults (process zones), far-field tectonic stresses, and insights from microfractures into the state of stress leading to earthquakes.

2. Historical context

Systematic observation of natural microfractures can be divided into an era dominated by transmitted light (TL) microscopy from ca. 1850 and an era after ca. 1960 when scanning electron microscopy (SEM) became a widespread tool. Another milestone was the application of cold cathode cathodoluminescence (Sipple, 1968) and SEM-based cathodoluminescence (CL) (Pagel et al., 2000) to the study of sealed microfractures.

In the early days of transmitted light microscopy, natural microfractures partly filled with mineral deposits were recognized in quartz-rich rocks (Fig. 1a). Sorby (1858) correctly inferred that alignments of minute inclusions in quartz-rich rocks are the relicts of small fractures. In a petrographic study of a conglomerate, Hicks (1884, p. 194) noted that "fracture-lines across the pebbles" were identifiable as "well-marked lines…formed in the presence of abundant vapours." He also noted that some "lines of fractures are also traceable from one fragment to another by thin strings of these secondary minerals," the first instance of the use of this basic crosscutting relationship to show that fractures or fluid-inclusion planes postdate the grains that contain them and are not features inherited from the source of the grain (Fig. 1b).

On scales visible to the unaided eye, inherited fractures are obvious, for example, to anyone observing veins in modern beach cobbles. So Hicks' comment likely reflects an appreciation that fractures in clastic rocks can be inherited. But on the microscale in siliciclastic rocks, relationships like the abrupt termination of vein material at rounded clast margins typically requires CL to detect (Fig. 1c and d; Laubach, 1997). Inherited fractures and inherited structural relations are, in fact, ubiquitous in sand grains and are readily documented with SEM CL (e.g., Boggs and Krinsley, 2006, p. 90). Particularly if coupled with inherited fluid–inclusion assemblage analysis, such microstructural indicators for paleotectonics and provenance have potential that has been largely neglected (Hooker and Laubach, 2007), probably partly because of early problems with color CL as a provenance indicator. But another reason may be a lack of appreciation within the provenance community of the value of the structural information that can be gleaned from the preserved crosscutting relations and other inherited structural features.

Following up these initial microfracture descriptions, the field of sandstone petrology has made productive use of microfracture observations. Grain fracturing was reproduced in compaction experiments (Borg and Maxwell, 1956; Maxwell, 1960; Borg et al., 1960; Friedman, 1963; 1969) and explained using grain-scale models (Gallegher et al., 1974; Wong et al., 1992; David et al., 1994). The advent of high-resolution CL (e.g., Fig. 1e and f) revitalized this research direction (Burley et al., 1989), helping to explain compaction, pressure solution, and the location and controls on cement distribution (Milliken, 1994; Dickenson and Milliken, 1995; Milliken and Laubach, 2000; Mork and Moen, 2007). CL revealed many more grain-contact microfractures than were visible using TL and showed that some features, such as lamellae and undulatory extinction and indented grains hitherto ascribed to crystal plasticity or pressure solution, were the result of microfracture, particle rotation, and quartz cementation (e.g., Milliken and Laubach, 2000, their Figs. 3–6). Most of these studies focus on issues of diagenesis rather than of structure. But grain-fracture and cementation ideas and imaging techniques developed in the sandstone diagenesis community are being applied to deformation bands where grain fracturing and concurrent cementation can occur (Milliken et al., 2005; Eichhubl et al., 2010) as well as to fault-rock studies (Fisher and Knipe, 1998; Fisher et al., 2003), as we discuss below.

Another closely related strand that can be traced back to early transmitted-light observations is the work within the fluid-inclusion community. Under transmitted light microscopy, some microfractures in quartz-rich rocks are marked by arrays of fluid inclusions (fluid-inclusion planes, FIPs) that can be analyzed as fluid-inclusion assemblages (Goldstein and Reynolds, 1994). Classified as secondary inclusions because they supposedly postdate the crystallization of the minerals that they crosscut, these features are widely used to recover temperature, pressure, salinity, and other compositional data (Roedder, 1984; Crawford, 1992). Fluid-inclusion-analysis methods have proven useful when adapted to structural analysis needs (Anderson and Bodnar, 1993). But this community tends to focus on geochemical challenges posed by the use of fluid inclusions, placing less emphasis on structural applications. Nevertheless, there is strong and increasingly active use of fluid-inclusion planes as structures and paleostress-direction indicators and as temperature and geochemical probes for unraveling fluid composition and migration/stagnation patterns in various burial settings in the context of structure and tectonics (Batzle and Simmons, 1976; Pêcher et al., 1985; Hay et al., 1988; Lespinasse and Cathelineau, 1995; Meere, 1995; Evans, 1995; Boullier, 1999; Lespinasse, 1999; Lespinasse et al., 2005; Hilgers et al., 2006; Travé et al., 2007; Fischer et al., 2009; Laubach and Diaz-Tushman, 2009; Becker et al., 2010; Fall et al., 2012).

2.1. Healed versus sealed microfractures

Hicks (1884, p. 195) concluded that microfractures were "… closed up by a secondary deposition of quartz". In his interpretation, the fluid-inclusion planes are merely small quartz-sealed veins, small versions of a type of structure familiar since the time of Hutton (Lyell and Deshayes, 1830). The challenge, however, is that under transmitted-light observation, fracture walls typically are invisible in microfractures filled mostly with quartz. In retrospect, this absence of discernibility is the result of the accumulation of quartz deposits exhibiting crystallographic and optical continuity with the quartz substrate – the same process that makes the

crosscutting relationships. After Hooker and Laubach (2007); see Laubach (1997) for classification criteria. (e) Transgranular fluid-inclusion plane (FIP), plane-polarized transmitted light. (f) Color SEM-CL of same area of (e), microfractures (MF), quartz cement (blue; red), Tulip Creek Sandstone, Ordovician Simpson Group, 4,085.5 m (13,404 ft) core depth, Grady County, Oklahoma. Both (e and f) are cut normal to bedding and the right-hand side is up for both images. Adapted from R. Reed and S. Laubach, 1996, and R. Reed, unpublished imaging 2005.Fracture walls are sharp; there is no evidence of the local dissolution step. (g) TL image of deformation lamellae from the same location as (a). The lamellae are the faint, thin subparallel features with a preferred up/down orientation. Also, a small number of FIP exist that dip at a low angle to the viewing direction in this photograph. (h) TL image of grain overgrowths from the Cambrian Tapeats Sandstone in southern Nevada. Many of the microfractures stop at the dust lines that define the original grain boundary, indicating they are inherited (from Anders et al., 2013).

Please cite this article in press as: Anders, M.H., et al., Microfractures: A review, Journal of Structural Geology (2014), http://dx.doi.org/10.1016/j.jsg.2014.05.011

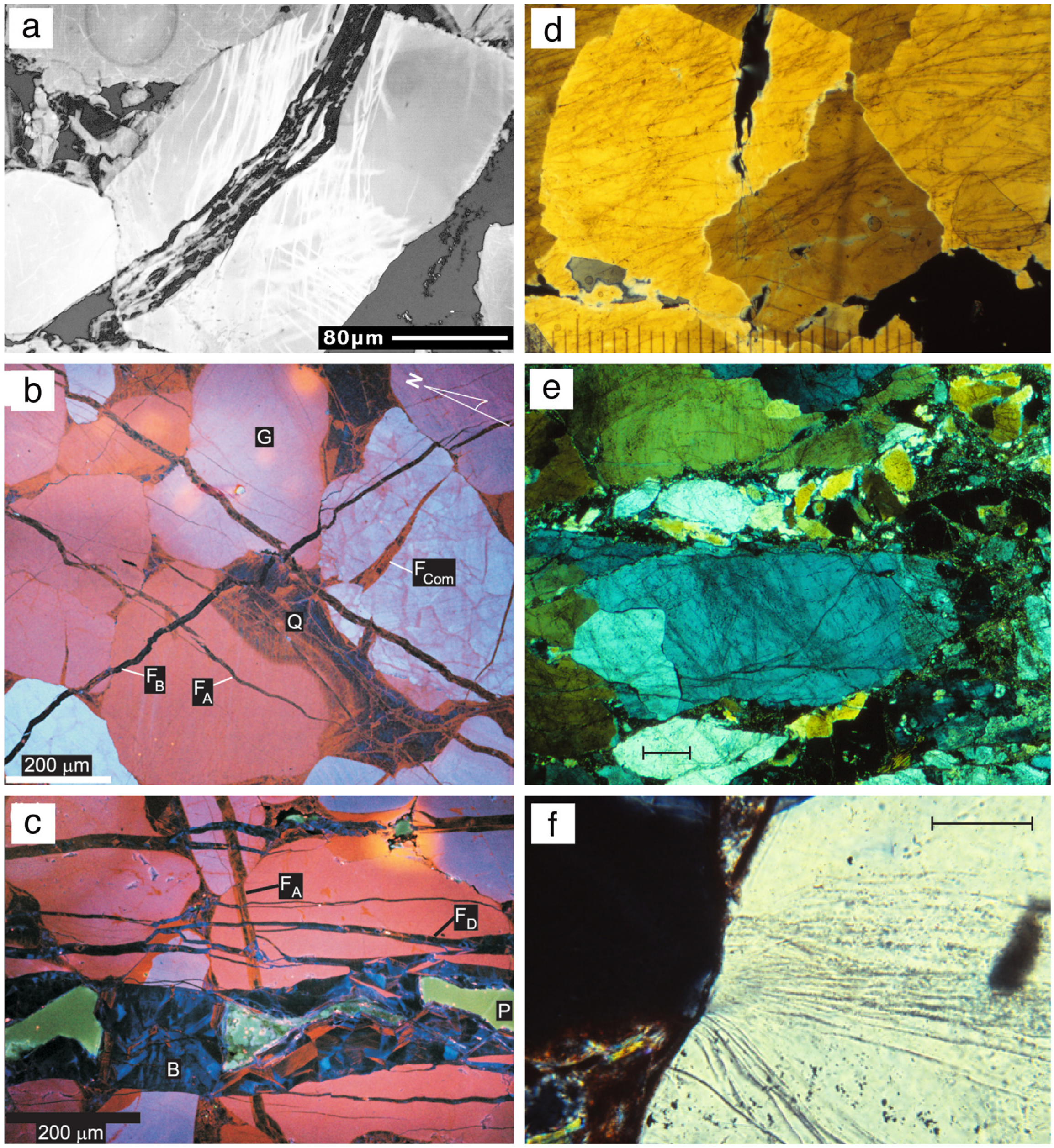

Fig. 2. (a) Crack-seal texture in microfractures. Panchromatic CL image, Pennsylvanian Pottsville Formation, Black Warrior Basin, Alabama, depth 1052.5 m. From Laubach et al. (2004a) (their Fig. 16b). (b) Crosscutting relations, sets F_A, F_B, and F_{Com} [compaction]. (G) grain. (c) Microfractures aligned with macrofractures and crosscutting relations, sets F_A, F_D, Cambrian Eriboll Formation sandstone, from Laubach and Diaz-Tushman (2009), 2b and 2c are their Figs 5a and 4b. (P) indicates preserved fracture porosity. In (c), (B) is a quartz bridge partially filling a microfracture. SEM-CL images, sections parallel to bedding (plan view; N, north direction). In sandstones, microfractures filled with quartz typically have lengths of a few to tens of millimeters and opening displacements (kinematic apertures) of 0.001 or less to 0.1 mm (Hooker et al., 2014). Width:length ratios (aspect ratios) vary considerably. (d) Microfractures (FIP) from a Tertiary Granite in the Mineral Mountains, west-central Utah, in transmitted light. Sample 200 m from the Cave Canyon detachment fault. The majority of microfractures are intragranular. Small tick marks are 100 μm. (e) Microfractures in the same granite as (d), located 12 m from the detachment. Note grain size reduction as the granite approaches the core of the fault. Scale bar is 360 μm. In transmitted light. (f). Microfractures (FIP) radiating from an impact point with an adjacent grain. Sample from the Fountain Formation near Boulder, Colorado. Scale bar is 100 μm. In transmitted light. From Anders and Wiltschko (1994).

boundaries between detrital quartz grains and quartz overgrowth cements difficult to distinguish in many sandstones (Fig. 1h). Thus the ambiguous appearance of fluid-inclusion planes permitted other interpretations. In granites, there was the possibility that primary crystallization played a role (Dale, 1923), an explanation for some microfractures borne out by subsequent work (e.g., Bouchez et al., 1992; Mancktelow and Pennacchioni, 2013).

Tuttle (1949) offered another explanation – crack healing – that remains the standard explanation for fluid-inclusion planes (Groshong, 1988, p. 1333; Passchier and Trouw, 2005, p. 284), but, as we will see, problems exist with this model. According to Tuttle, the starting point is a liquid-filled fracture. But the next step of the postulated healing process involves local-scale (that is, within the fracture walls) dissolution, diffusive mass transfer, and nearby dendritic precipitation of quartz. The "process of solution and deposition" results in large, thin, sheet like inclusions having an extremely irregular outline: "…continued differential solution and deposition of silica gradually change the shape of the individual inclusions from thin sheets to more nearly equant bodies." Eventually individual inclusions grow, and they may have diameters larger than the initial fracture width. The time-dependent process is supposed to result in such distinct sizes and shapes of inclusions that Tuttle postulated that these attributes could be used to assess the age of the structure. Differences in fluid-inclusion shapes and sizes are readily apparent in TL images (Fig. 1a and b).

Subsequent creation of fluid-inclusion planes in the laboratory seemed to confirm Tuttle's interpretation, inasmuch as the fluid-inclusion planes form readily from fluid-filled microcracks; nevertheless, the experimentalists noted that laboratory microfracture closure could have resulted by deposition of material transported over distances greater than grain scale, in other words, by a process of sealing (Lemmlein and Kliya, 1960; Smith and Evans, 1984; Brantley, 1990; Brantley et al., 1990). Microfracture sealing can be an extremely rapid process (Lander and Laubach, 2014), although sealing of wide fractures can be slow (Becker et al., 2010).

A key marker of the healing process should be textural evidence of dissolution on microfracture walls (Laubach, 1989). The healing process, as described by Tuttle, involves dissolution of the fracture wall rock (that is, local, within-the-fracture dissolution). This should be evidenced in CL as a pitted (dissolution) texture or a fracture–wall mismatch. The healing model predicts that the fracture walls should not be sharp.

SEM CL analysis shows that quartz-filled microfractures in sedimentary and low-grade metamorphic rocks have sharp walls, whether or not fluid inclusions are present. Healing processes cannot be ruled out for all fluid-inclusion planes, particularly those in rocks deformed at high temperature that lack CL contrasts, or where heating subsequent to fracture closure has erased CL contrasts so that fracture walls cannot be distinguished. But SEM CL analysis of fluid-inclusion planes in most granites, most metamorphic rocks, and a wide cross section of sedimentary rocks (Fig. 1) shows that Hicks was right; fluid-inclusion planes are microveins. A distinction between healed and sealed microfractures on the basis of criteria such as the presence or absence of fluid inclusions (Mizoguchi and Ueta, 2013) is probably not fundamental. Cement textures within fractures are typical of those in larger veins; these textures are markers for precipitation in open cavities, and, in some cases, for recracking (crack-seal texture; e.g., Ramsay, 1980) (Laubach, 1997; Laubach et al., 2004a; Fig. 2a). Fluid inclusions are generally much smaller than those in quartz-filled micro-veins and fit well within the confines of veins defined by fracture walls. Fluid inclusions are commonly trapped along medial lines (showing that they really are primary inclusions after all) and their shapes do not reflect fracture aging except inasmuch as older microfracture arrays tend to be more thoroughly cemented with quartz (Laubach and Diaz-Tushman, 2009) as a natural consequence of thermal exposure in sedimentary-basin environments (Walderhaug, 1994; Lander et al., 2008). Some studies that used transmitted-light images of FIPs to determine the size and shape of fractures, on the premise that the inclusion distribution and widths are adequate proxies for fracture-opening displacement (Onasch, 1990), are not validated. Nevertheless, for microfractures with apertures in the range of 1 micron or less (Onasch, 1990), new approaches for discriminating healing and sealing processes should be sought (Onasch and Vennemann, 1995; Onasch et al., 2009).

The inference, on the basis of early experimental results, that the presence of open microfractures implies relatively low temperatures and recent (young) fractures (Kowallis et al., 1987; Laubach, 1989) has been borne out by more-recent experiments and cement-growth modeling (Lander et al., 2008; Lander and Laubach, 2014) as well as by cement accumulation records tied to burial histories by fluid-inclusion analysis (Becker et al., 2010; Fall et al., 2012). Fluid-inclusion planes should be referred to as quartz-filled (or quartz-lined) microfractures unless definitive evidence of either healing or sealing can be adduced.

2.2. Microfractures in quartz-rich rocks

In the study of quartz-rich rocks there is a tradition, traceable back to Tuttle (1949) and his contemporaries, of continuous research on fluid-inclusion planes (interpreted to be microfractures) (Riley, 1947; Tuttle, 1949; Bonham, 1957; Roberts, 1965; Wise, 1964, 2005; Harper, 1966; Friedman, 1969; Engelder, 1974; Simmons and Richter, 1976; Brock and Engelder, 1977; Pêcher et al., 1985; Lespinasse and Pêcher, 1986; Kowallis et al. 1987; Jang et al., 1989; Laubach, 1989; Ren et al., 1989; Anders and Wiltschko, 1994; Lespinasse, 1999). Many of the early studies, including Tuttle's, addressed or were focused on other microstructures in quartz, such as deformation lamellae (Fig. 1g). Some of these papers (i.e., Tuttle, 1945; Ingerson and Tuttle, 1948; Tuttle, 1949) are also antecedents to current work on the microstructures of crystal plasticity. It is possible that Tuttle himself (had he known of it) might have objected to the term "Tuttle lamellae" (Groshong, 1988) for fluid-inclusion plane arrays, on the grounds that he recognized fluid-inclusion planes to be quartz-filled fractures formed by a brittle process, in contrast to the other lamellae formed by nonbrittle processes in the same rocks.

2.2.1. Cathodoluminescence of quartz-filled microfractures

The systematic application of cathodoluminescence, and in particular SEM-based CL, marked a fundamental advance over the use of transmitted light observations in the study of quartz-filled microfractures. In addition to resolving how these features form, as discussed above, in many rocks CL reveals the boundaries (or walls and tips) of fractures in sharp detail, in part because of differences in luminescence between host quartz and quartz within the fracture (Fig. 1d and f). Typically, CL reveals many more microfractures than are apparent as fluid-inclusion planes, demarcates opening displacements and lengths, reveals crosscutting or abutting relations, and allows more meaningful description of any cavities (open pore spaces) within fractures (Fig. 2b and c). In some cases, evidence of multiple stages of fracture opening can be found in cement textures (Laubach, 1997; Laubach et al., 2004a, their Figs. 3 and 14). Consequently, fluid-inclusion planes can be more confidently identified as fractures and are more useful for structural analysis (Sprunt and Nur, 1979; Kanaori, 1986; Narahara and Wiltschko, 1986; Boiron et al., 1992; Lloyd and Knipe, 1992; Knipe and Lloyd, 1994; Milliken, 1994; Laubach 1997; Laubach and Ward, 2006).

These benefits were not so apparent with early CL devices (Sipple, 1968; Sibley and Blatt, 1976), but improved resolution, color imaging, and SEM-stage automation enables sharp microstructural definition (Milliken and Laubach, 2000) over wide areas, in some cases encompassing image strips across tens of thin sections (Gomez and Laubach, 2006; Hooker et al., 2009). A limitation of CL analysis, compared to transmitted light microscopy, is that CL essentially provides a map of the sample surface, so 3D information, such as the dip of fractures, needs to be acquired using either multiple thin sections in different orientations, or else sequential sections. Tuttle (1949) and other early workers used the universal stage to measure microfracture orientations, but features dipping less than 45 degrees are in a blind spot and cannot be measured accurately. This problem can be overcome by using dip information and optical measurements from precisely measured sections (Simmons et al., 1975; Simmons and Richter, 1976; Boullier and Robert, 1992), using an adaptation of the spindle stage for more accurate measurement of 3D orientation (Anderson and Bodnar, 1993), or simply using mutually perpendicular-cut thin sections with a universal stage with sweeps down to 45° and combining results (Anders, 1982; Anders and Wiltschko, 1994). Nevertheless, TL techniques are difficult for large-area analysis, and recent CL-

Please cite this article in press as: Anders, M.H., et al., Microfractures: A review, Journal of Structural Geology (2014), http://dx.doi.org/10.1016/j.jsg.2014.05.011

based approaches have used multiple image types, including transmitted light, layered in image-analysis software (Fall et al., 2012) but with some loss of 3D-orientation rigor.

2.3. Microfractures in non-quartz-rich rocks

The potential for the use of pervasive fluid-inclusion planes—microfractures—as tracers of past deformation patterns and conditions was appreciated at an early stage (Riley, 1947; Tuttle, 1949), and these structures are recognized low-temperature microstructures (Groshong, 1988; Passchier and Trouw, 2005). But this fluid-inclusion plane/microfracture literature has been almost exclusively focused on quartz-rich rocks: quartzites, granites, and quartz-rich metamorphic rocks. Before tracing this productive research direction, it is informative to consider the presence (or absence) of microfractures in other rock types. Although experimental microfractures are typically created in a wide range of rock types, there is no tradition of systematic study of natural microfractures in dolostones, limestones, or shales (mudrocks). In coal, a wide range of fracture size, including microfractures, has long been recognized, but the microfracture component of coal fractures (cleats) is rarely explicitly described (Laubach et al., 1998). In dolostones, microfractures are widespread, but until recently notice of these structures was mostly as a component of diagenesis studies (Kupecz and Land, 1991; Montanez and Read, 1992; Marquez and Mountjoy, 1996), despite the widespread view that dolostones are fracture prone and indeed form fractured reservoirs for petroleum and ore deposits (Nelson, 1985; Davies and Smith, 2006). The advent of size-scaling studies, discussed later, has brought systematic description of microfractures (with apertures down to 1 μm) and more attention to the full range of fracture sizes in dolostones (Gale et al., 2004; Ortega et al., 2006; Hooker et al., 2012a) and limestones (Gale, 2002; Marrett et al., 1999; Gomez and Laubach, 2006).

Shales or mudstones are surprising because they apparently lack pervasive or disseminated microfracture populations. These rocks are a special case because of their current economic importance. Because some production amounts from low-permeability gas-bearing shales have been interpreted to be too large to be explained by gas from the shale matrix, analysts infer an open microfracture network contributing to permeability (Apaydin et al., 2012). But as Gale et al. (2014) note, the theorized microfractures that these engineering studies posit could be on the centimeter- to decimeter- (or more) length scale, given petroleum engineering (and geophysicist) usage, and thus outside our definition. Microfractures do occur in shales but are uncommon if, by "microfracture," we mean, in the geologic sense, a fracture a few microns wide and a few millimeters in height or length. Examples include bitumen-filled microfractures in Devonian Catskill shales (Lash and Engelder, 2005) and Oligocene Frio Formation shales (Capuano, 1993). Some of these fractures are barren and could result from core disaggregation or outcrop weathering. Gale et al. (2007) found few fractures <30 μm wide in the Barnett Shale and Austin Chalk (silica-rich and carbonate-rich fine-grained rocks, respectively). In a survey of shale fracture data from many active shale-gas plays, Gale et al. (2014) found most shale-fracture apertures in the size range of between 30 μm and 1 mm, with size ranges for individual formations or core sets mostly narrower. The upper aperture sizes are comparable to those in dolostone and sandstone, but the lower limit for shales is higher, a few tens of microns, and Gale et al. do not see many fractures below this size in shales. The overall patterns resemble size-restricted patterns found in some limestones (Gale, 2002) and dolostones (Hooker et al., 2012a), as well as in sandstones that lack microfracture populations that have shale-like mechanical properties and composition (Ellis et al., 2012) or fractures that formed under conditions of low temperatures and low cement accumulation volumes (including barren joints) (Hooker et al., 2013). Gale et al. suggest that microfractures in shales may be more prevalent than these observations suggest, but at such low abundances that they are usually not sampled. The apparent lack of pervasive microfractures in some rocks, including shales, and their prevalence in other rocks (at least for fracture arrays formed under certain conditions) remains to be explained. Some suggestions have been posited (Hooker et al., 2013), which we discuss later.

3. Formation of microfractures in rock

3.1. Mechanics of Mode I cracks in rock

The modern theory of brittle fracture was initiated by Griffith (1920). His theory was in the form of an energy balance, in which he solved for the energetic conditions necessary for the propagation of a crack. During the 1950s, primarily due to the work of Irwin (1958), a formalism was developed - Linear Elastic Fracture Mechanics – that lends itself to the solution of general crack problems.

In this model, a crack is assumed to be a mathematically sharp slit embedded within an elastic medium. Three modes of cracking are defined. Mode I is the opening mode and Modes II and III are the two shear modes. Here we will be concerned primarily with Mode I cracks, sometimes called tensile cracks, in which the displacements of the crack walls are normal to them. For this mode, the maximum aperture $D_{\max}$ between the crack walls is related to crack length L by

$$D_{\max} = \Delta\sigma \frac{(1-\nu)}{\mu} L \tag{1}$$

where μ is rigidity, ν is Poisson's ratio, and the effective driving stress $\Delta\sigma = (\sigma_n - p)$ is the difference between the applied stress normal to the crack wall and the pore pressure within the crack. The minus sign appears because a positive opening corresponds to a negative effective stress (tension).

The stresses near the tip of the crack are

$$\sigma_{ij} = K(2\pi r)^{-1/2} f_{ij}(\theta) \tag{2}$$

where r is the distance from the crack tip, K is the stress-intensity factor, and $f_{ij}(\theta)$ are functions that describe the dependence of each stress component on the angle θ from the plane of the crack. The stress-intensity factor for an isolated crack is given by

$$K = \Delta\sigma \left(\frac{\pi L}{2}\right)^{1/2} \tag{3}$$

Griffith assumed that the crack would propagate when the energy released in propagating the crack was just sufficient to supply the surface energy to create the new crack increment. This criterion is incorporated in fracture mechanics by assuming that the crack propagates when K reaches a critical value K_c defined by when the energy release rate G attains a critical value G_c equal to the increment of surface energy necessary to break the bonds at the crack tip,

$$G_c = K_c^2 \Big/ 2(1+\nu)\mu = 2\alpha \tag{4}$$

where α is the specific surface energy, a property of the material. Thus during propagation, $K = K_c$, a constant, and Eq. (3) shows that the driving stress $\Delta\sigma$ will decrease as the crack lengthens, i.e. the crack weakens as it lengthens. Such a crack would thus be unstable under constant stress boundary conditions. The Griffith energy balance states that this instability will occur when the crack reaches a critical length L_c, given by

$$L_c = \frac{8\mu(1+\nu)\alpha}{\pi T^2} \tag{5}$$

where T is the tensile strength of the rock. Under the constant stress boundary conditions assumed by Griffith, when a crack reaches this critical length, it will propagate without limit. Evaluating Eq. (5), assuming $\mu = 20$ GPa, $T = 5$ MPa and α from experimental data is 10–100 Jm^{-2} (Hoagland et al., 1973) provides estimates of L_c between 2.5×10^{-2}–2.5×10^{-1}m.

Combining Eq. (1) with Eq. (3) we obtain

$$D_{\max} = \frac{(1-\nu)}{\left(\sqrt{\pi/2}\right)\mu} K_c L^{1/2} \tag{6}$$

which predicts that $D_{\max}$ scales as $\sqrt{L}$.

According to this theory, fracture will occur when the longest, most favorably oriented crack becomes critical. This assumes a homogeneous material. Because of the granular nature of rock, stresses in rock are highly heterogeneous at the grain scale. As a result, when rock is loaded in tension in the laboratory, acoustic emissions from the propagation of many microfractures are observed prior to the formation of the macrofracture that leads to the final failure of the specimen. This failure is the result of the coalescence of microfractures (Mogi, 1962; Zeitlow and Labuz, 1998; Tham et al., 2005). As will be described later, the same behavior is observed in compression tests (see Horii and Nemat-Nasser, 1985). This pattern leads to the phenomenon that is the subject of this article: microfractures at a wide range of scale lengths are commonly found in many rocks.

For shear-mode cracks (faults), multiple observers have found that $D_{\max} \propto L$, in agreement with Eq. (1) and not Eq. (6) (Cowie and Scholz, 1992; Dawers et al., 1993; Schlische et al., 1996). This implies that $K_c \propto \sqrt{L}$ and thus $G_c \propto L$, contradicting the assumption of Griffith. The reason for this behavior again lies in the heterogeneity of rock: macrocracks coalesce and propagate within a volume of intense microfracturing, called a process zone (e.g., Atkinson, 1987). Thus the surface energy required to propagate the macrocrack (fault) involves not only the new surface area of that crack, as Griffith assumed, but all the microcracks in the process zone that are integral to the formation of the macrocrack. Because the size of the process zone is found to grow proportionally to the length of the fault (Vermilye and Scholz, 1998; Faulkner et al., 2011), the fracture energy, $G_c \propto L$. Realizing that $K_c \propto \sqrt{L}$ we see from Eq. (3) that faults grow at a constant stress drop, scaling according to Eq. (1). The finding that $G_c \propto L$ means, from Eq. (5), that there is no longer a Griffith instability or critical length. Cracks are thus stable under constant stress boundary conditions.

Subsequent work has shown that the same conclusions may be made for Mode I fractures in rock – joints, veins, and dikes. A study of the scaling law for veins found a linear relationship between $D_{\max}$ and L (Vermilye and Scholz, 1995). It had been long known from laboratory experiments that Mode I crack propagation is associated with a growing process zone (Swanson, 1987; Labuz et al., 1987). More recent work, discussed in a later section, showed that the process zones grow linearly with fracture size, just as in the case with faults. Hence, Mode I fractures in rock scale linearly with L for the same reason as do faults.

However, there is a school of the study of Mode I fractures in rock that has proceeded along classical linear elastic-fracture mechanics lines in which the Griffith assumption is implicit. Segall (1984), for example, recognized the existence of sets of joints with greatly varying lengths that evidently grew quasi-statically and must therefore be incompatible with the Griffith instability. He thus proposed that joint sets grow under constant displacement-boundary conditions. This idea would preclude the possibility of horizontal joint sets, because the vertical stress, being produced by the weight of the overburden, is a body force and manifestly results in constant stress boundary conditions.

Olson (2003) argued, along the lines of Eqs. (1)–(6), that $D_{\max}$ must scale as $\sqrt{L}$ rather than as L, and, while other analyses support this view (Schultz et al., 2008), other ways exist for handling and interpreting the data (Scholz, 2010; Olson and Schultz, 2011; Scholz, 2011; Schultz et al., 2013). Because of stress interactions between the segments of en echelon arrays, these arrays may exhibit scaling of the form $D_{\max} \propto L^{1/n}$ where n is greater than 1 (Pollard et al., 1982; Vermilye and Scholz, 1995; Olson, 2003) so that the scaling of such multisegment arrays often is closer to $\sqrt{L}$ than L. To advance the discussion of reconstructions of fracture shape histories from inception as microfractures would be a useful direction for future research, and one now feasible in certain rock types (Becker et al., 2010).

3.2. Experimental stress-induced microfractures

Microfractures (microcracks) induced under experimental conditions provide important information about the processes of failure in rock and lead to a better understanding of faulting and the formation of microfractures in nature (Scholz, 2002). The development of experimentally induced microfractures was first demonstrated where dilatancy was observed in triaxial compression tests (Brace et al., 1966). The dilatancy is manifest as inelastic expansion normal to the σ_1 direction, from which researchers have deduced that the dilatancy was produced by the growth and opening of Mode I microfractures (dilatant microcracks) parallel to σ_1. That this process involved the growth of new cracks was demonstrated by acoustic-emission studies (Scholz, 1968a, b; Lockner et al., 1991; Reches and Lockner, 1994). True triaxial compression tests show that, when $\sigma_3 < \sigma_2$, the dilatant microcracks are oriented preferentially in the σ_1–σ_2 plane (Mogi, 1971) or somewhat obliquely to them (Healy et al., 2006a; 2006b). Dilatant microcrack anisotropy may also be caused by anisotropic rock fabric (Scholz and Koczynski, 1979). Microscopic examination of samples deformed in the laboratory confirmed these conclusions. Note that microfractures can often be inferred to nucleate at grain boundaries (Gallegher et al., 1974; Tapponnier and Brace, 1976; Kranz, 1979, 1983b; Wong 1982; Moore and Lockner, 1995; Homand et al., 2000; Katz and Reches, 2004). Stress cycling results in the opening and closing of dilatant microcracks along hysteresis loops (Scholz and Koczynski, 1979; Scholz and Hickman, 1983).

Although much has been learned in the laboratory, most experimental work on microfractures does not include concurrent chemical processes (such as cement precipitation) that, as shown by observation of microfracture populations, operate in many settings in the Earth. In subsurface environments, rock and fault properties, for example, may change during deformation as a result of cement precipitation. Cement deposition may affect whether and how microfractures evolve into larger fractures, with consequences for fracture-size scaling (Clark et al., 1995; Hooker et al., 2012a). A new generation of experimental work may be needed to fully address these and other issues.

3.3. Microfracture size distributions

Like macrofractures, microfractures occur in sets, or populations, that exhibit well-defined statistical properties such as their size distribution. This distribution has been observed as exponential (Snow, 1970; Baecher and Lanney, 1978) but more commonly as a power-law distribution (Gudmundsson, 1987; Barton and Zoback, 1992; Clark et al., 1995; Gross and Engelder, 1995; Loriga, 1999; Marrett et al., 1999; Ortega and Marrett, 2000; Gillespie et al., 2001; Laubach and Ward, 2006; Ortega et al., 2006; Davy et al., 2010; Guerriero et al., 2010; Hooker et al., 2009; 2011; Hooker et al., 2014). However, in many cases, particularly with small data sets, the type of distribution is not clear-cut. The measured quantity in microfractures is usually opening displacement (kinematic aperture), but because aperture may scale linearly with length (Vermilye and Scholz, 1995; cf. Olson, 2003; Schultz et al., 2008), aperture size distributions could be proxies for length distributions. Why such scaling arises (or fails to arise) in microfracture populations is an area where more work is needed. Observational studies that document microfracture lengths, test models of how microfracture aperture and length relate, and the question of whether and how such patterns evolve across the entire fracture size range constitute another topic where more data is needed. Advanced imaging procedures allow such experiments to probe microfracture growth in ways that were not possible previously (Barnhoorn et al., 2010).

Power-law distributions are typical of fractal objects that exhibit self-similarity, and such distributions are continuous over a scale range for which no characteristic dimensions exist. In nature, such distributions are truncated at characteristic dimensions of the system, either by a transition to another fractal state, characterized by a change in the exponent in the power-law, or by an upper or lower fractal limit (Scholz, 1995; Marrett, 1996). Two such characteristic length scales in rock merit discussion: the grain size and, for sedimentary rocks, the mechanical-layer thickness.

Because rock is a polycrystalline aggregate of one or more crystal phases, many of which are anisotropic in their physical properties, stresses within the rock will be heterogeneous at the grain scale, owing, in crystalline igneous and metamorphic rocks, to the mismatch between elastic and thermal–elastic properties of adjacent grains, and in porous clastic rocks, to contact stresses between adjacent grains. Therefore noise exists in the stress field at the grain scale in crystalline rock, and it is at this scale that stress concentrations exist that can nucleate and propagate microfractures, even though the regional stresses are well below the fracture strength of the rock. This pattern implies that the nature of the microfracture population will depend on the fabric of the rock. For polyphase igneous or metamorphic rocks, such as granite, there exists high contrast between grains in physical properties like elasticity and thermal expansion as well as a high degree of grain interlocking. This geometry results in high stress concentrations and hence high densities of grain-boundary and intragranular cracks. For monomineralic, crystalline rocks such as marble or peridotite, where property contrasts are less than in other rocks, microfracture density may be less as well. For clastic rocks such as sandstone, grain-contact stresses are dominant at low levels of diagenesis (low compaction or cement content) and intragranular microfractures emanating from contact points are common (Fig. 2f). The presence of cement progressively supports transgranular stresses so that stress concentrations at grain boundaries become muted and microfractures become less concentrated at grain boundaries. Rocks such as mudstones and shales, on the other hand, contain phyllitic minerals, especially clay, in their matrices; these phyllitic minerals may act ductily to suppress cracking.

Although smaller microfractures can be detected (Gomez and Laubach, 2006), studies of microfracture kinematic-aperture size distributions typically have a lower resolution limit of about 10^{-3} mm, which, using an aspect ratio of 1000 (Vermilye and Scholz, 1995), indicates microfracture lengths of about 1 mm. This is close to or larger than the grain size of the rocks studied, typically medium- to very fine-grained sandstones; hence any aperture transition at the grain scale is not readily measurable with current imaging methods. Hooker et al. (2009), in a study of sandstone, found that most microfractures were intragranular, whereas only transgranular microfractures could be confidently ascribed on textural grounds to the same population as macrofractures. The aperture distribution at the small scale was best fit with a log-normal distribution, suggesting that a lower cut-off was being sensed or that at the grain scale and smaller, populations of differing origins are present but indistinguishable (Laubach, 1997). In a study of experimentally deformed granite, however, Katz and Reches (2004) observed that microfractures follow a power-law distribution that peaks at the grain scale and shows a rapid cutoff in microfracture abundance below that scale. These observations suggest that a lower fractal limit exists, occurring at the scale of the grain size in many rocks.

For large fractures, mechanical layer thickness can affect fracture height growth, for example where there is a marked contrast of competency or ductility between layers so that fractures are bound within the more brittle layers. Such bed-confined fractures may be of equal height and aperture and regularly spaced, having a spacing that is proportional to the layer thickness (Price, 1966, p. 144). In this instance, the spacing of these fractures is proportional to layer thickness because it is the latter that controls the width of the stress shadow of a crack of that height (Hu and Evans, 1989; Bai et al., 2000). Field observations and geomechanical models that simulate fracture propagation suggest that even for strata-bound fractures, fracture arrangement can be more complicated than this (Olson et al., 2009 and references therein). Moreover, complex hierarchies of large fracture heights exist but have yet to be adequately described and classified (Hooker et al., 2013), and mechanical layering itself commonly evolves through time (Laubach et al., 2009). How these patterns of large fractures and the enclosing mechanical stratigraphy evolve, and how this evolution relates to the growth of microfractures and the development of size scaling, are areas that could be addressed with new observational, experimental, and modeling work.

Some numerical experiments give promise of convergence between models and observations. Spyropoulos et al. (1999b) studied a numerical model of the spontaneous growth of fractures in an elastic layer. They found three regimes. At low strains, the fractures behave independently and form a power-law distribution. At higher strain, where fracture interactions become important in inhibiting nucleation of new fractures and forming longer fractures by coalescence of smaller fractures, this distribution becomes warped into an exponential distribution. The system finally saturates at high strain into a system of equally spaced system-size cracks. The transition with strain from a power-law to exponential distribution was replicated in a physical model (Spyropoulos et al., 1999) and also observed in field data (for faults) by Gupta and Scholz (2000). The exponent for the power-law frequency distribution found in the model was about −2. This corresponds to an exponent of −1 in a cumulative distribution, which is similar to the values of about −0.8 to −1.0 observed for microfractures (Marrett et al., 1999; Ortega et al., 2006; Hooker et al., 2014). Numerical experiments that replicate fracture growth by rules that mimic inhibition of fracture growth by cement accumulation also

Please cite this article in press as: Anders, M.H., et al., Microfractures: A review, Journal of Structural Geology (2014), http://dx.doi.org/10.1016/j.jsg.2014.05.011

can produce values in this range (Clark et al., 1995; Hooker et al., 2012a).

4. Paleostress

4.1. Microfractures formed by unroofing

Igneous and metamorphic rocks have fabrics of closely interlocking crystals. When such rocks are unroofed – taken to pressures and temperatures lower than that at which they crystallized – internal stresses will be induced at the grain scale due to mismatches between grains of their elastic and thermal–elastic properties. These stresses will produce microfractures that occur primarily along grain boundaries (Kanaori et al., 1991; Vollbrecht et al., 1991; 1999; Kruhl et al., 2013). These microcracks, though typically resulting in porosities well below 1%, play an important part in rock properties, forming a continuous crack network and hence playing a leading role in the rock's transport properties, such as electrical conductivity (Brace and Orange, 1968) and permeability (Kranz et al., 1979; Walsh and Brace, 1984).

4.2. Microfractures and tectonic stresses

Early studies of fluid-inclusion planes (sealed microfractures) demonstrated a relationship between their orientation and that of local folds (parallel and perpendicular to some fold hinges; Riley, 1947; Bonham, 1957) and faults, thus establishing the value of these fluid-inclusion planes for the assessment of paleostresses (e.g., Tuttle, 1949). The orientation of open microfractures is indicative of stress directions at the time of their formation, so fluid-inclusion planes that form rapidly from microfractures are good paleostress indicators. The orientations of fluid-inclusion planes are not necessarily aligned with the present state of stress (as is also the case for some open macrofractures, Laubach et al., 2004b). Rocks commonly contain several fluid-inclusion plane sets, reflecting differences in stress orientation over geologic history (e.g., Dezayes et al., 2000; Laubach and Diaz-Tushman, 2009; Figs. 1a–d, h, 2b–e). The key to unlocking paleostress-trajectory histories and using these structures as paleotectonic indicators is determining the timing of these arrays, which can be accomplished in some cases using crosscutting relations, fluid-inclusion trapping temperatures, evidence of thermal history, and kinematic-compatibility arguments (Laubach and Diaz-Tushman, 2009). Few such studies have been published, but the potential exists for refining timing arguments and improving the use of fluid-inclusion plane arrays as a tectonic indicator to augment paleotectonic analysis (Boullier, 1999). Fluid-inclusion planes may record fracture opening (Laubach, 1988b), paleoseismic events (Boullier and Robert, 1992), the character of fluids in deformational settings (Pêcheret al., 1985; Cathelineau et al., 1990; Boullier, 1999; Lespinasse, 1999), and, assuming inclusion size is a marker for microfracture opening displacement, finite strain (Onasch, 1990).

Geologic studies of documentable – or fossilized – microfracture arrays shows that their formation in rock is not constant. For example, Laubach and Diaz-Tushman (2009) show that, over a span of about 500 m.y., only five microfracture sets formed in the Cambrian Eriboll sandstone in NW Scotland, despite a complicated loading history. Adjacent Precambrian sandstones are almost devoid of microfractures (Ellis et al., 2012), despite having gone through the same loading history plus an additional, eventful 400 m.y. Despite the stress cycling experienced by these rocks, the microfracture record, while informative, does not include every shift in tectonic load. Microfractures have been postulated to account for seismic anisotropy (Sayers and Kachanov, 1995), which may arise from contemporary stress fields (Crampin, 1987, 1994; Marrett et al., 2007; Rempe et al., 2013), but the geologic evidence that microfractures form intermittently (and not for every paleostress state) and readily seal (and thus are likely to provide only ephemeral seismic signals) suggests problems with this concept as currently formulated.

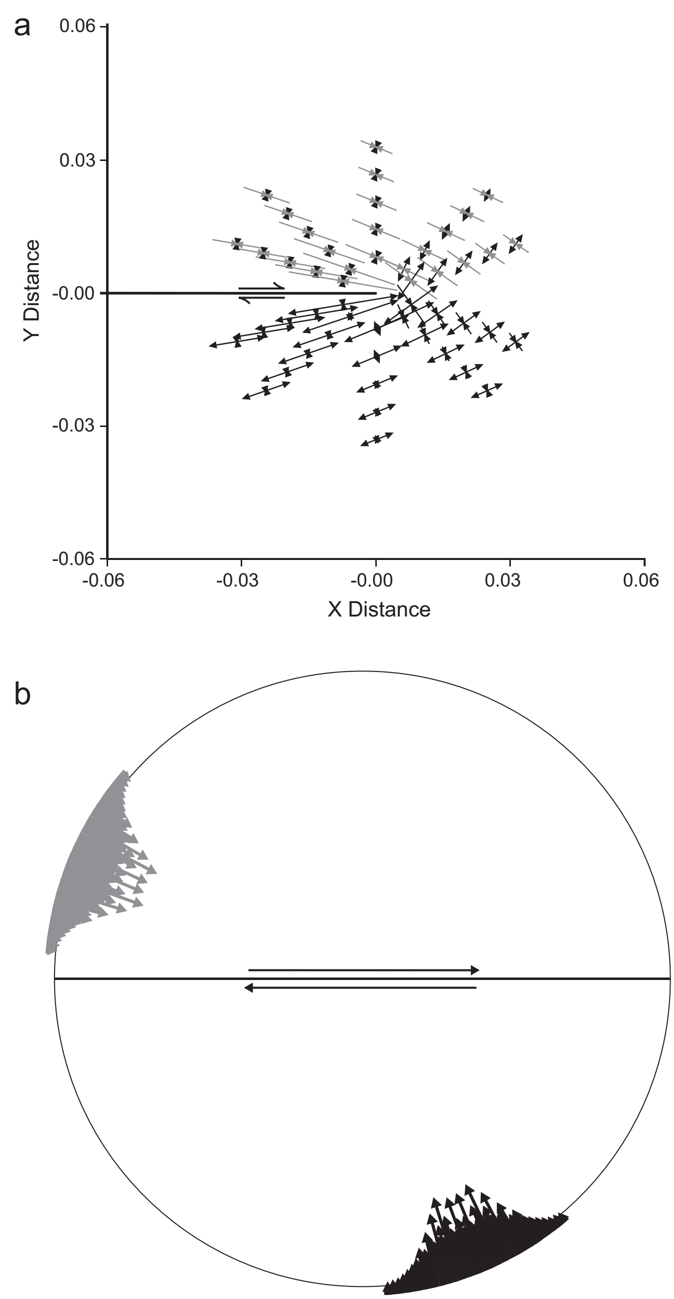

Fig. 3. Modeling of the stresses and fracture orientations surrounding a Mode II propagating fault (modified from Scholz et al., 1993). (a) Predicted orientation of stresses surrounding the tip of a Mode II fault. For positive *Y* values all inward pointing gray arrows represent the orientation of the maximum principal stress direction. For negative *Y* values black inward pointing arrows represent the maximum principal stress direction. Short black inward pointing arrows for positive *Y* values and all outward pointing arrows represents the least principal stress direction. (b) The orientation of Mode I fractures based on stress orientations determined from the model used to calculated in (a). The length of the arrows represents the relative proportion of the predicted Mode I fractures having that orientation (fault motion direction is represented by the two long single-sided arrows paralleling the equatorial line representing the fault surface).

Please cite this article in press as: Anders, M.H., et al., Microfractures: A review, Journal of Structural Geology (2014), http://dx.doi.org/10.1016/j.jsg.2014.05.011

Fluid-inclusion planes have been used as indicators of paleostress directions in a variety of rock types, including metamorphic rocks (Tuttle, 1949), deformed sedimentary rocks (Engelder, 1974; Knipe and White, 1979; Dula, 1981; Anders, 1982; Mitra, 1987; Laubach, 1988a,b; Onasch, 1990; Anders and Wiltschko, 1994; Vermilye and Scholz, 1998; Wilson et al., 2003; Iñigo et al., 2012; Anders et al., 2013), and less deformed or largely undeformed sedimentary rocks in a wide range of settings (Laubach, 1989; 1997; Laubach and Ward, 2006; Laubach and Diaz-Tushman, 2009). Building on observations of regional patterns of strength anisotropy in New England granites (Tarr, 1891; Dale, 1908; 1923), researchers have documented fluid-inclusion plane arrays in igneous rocks in laboratory experiments and inferred the fabric to record regional stress patterns (Nur and Simmons, 1970; Holzhausen, 1977; Plumb et al., 1984; Lespinasse and Pêcher, 1986; Hall, 1987; Kowallis et al., 1987; Ren et al., 1989; Fleischmann, 1990; Vollbrecht et al., 1991; Anders et al., 2001; Nadan and Engelder, 2009). The value of such studies is increased where strength and other laboratory tests are combined with microstructural and fluid-inclusion analysis to constrain timing of the microstructural fabrics.

4.3. Microfractures and fault zones

Faults (shear cracks) are inherently macroscale features. Faults formed by the coalescence of Mode I microcracks (Scholz, 1968b; Lockner et al., 1991) and propagate via a cloud of microfractures formed in the stress concentration at the fault tip; when crack density reaches a critical value, this cloud of microfractures breaks the rock down into a cataclasite that allows shear displacement to occur (Cowie and Scholz, 1992). The orientations of microfractures in the process zone reflect the fault-tip stresses rather than the regional stresses (Fig. 3; Scholz et al., 1993; Vermilye and Scholz, 1998; Suzuki, 2012). In the wake of the process zone, the passage of the fault tip leaves behind a damage zone of microfractures with a width that scales with the length and displacement of the fault (Vermilye and Scholz, 1998; Savage and Brodsky, 2011; Faulkner et al., 2011).

Faults are not planar features but have irregular traces (waviness) that can be described as fractal topography (Aviles et al., 1987; Power et al., 1987). As fault slip accrues, geometrical irregularities impinge on one another. Stress concentrations from these interactions produce additional microfractures in the surrounding rock with a different orientation than those formed in the process zone (Chester and Chester, 2000; Wilson et al., 2003; Faulkner et al., 2011). The total damage zone of the fault consists of microfractures produced by both mechanisms.

4.4. Microfracture density in the damage zones of faults

Brock and Engelder (1977) demonstrated that surrounding the Muddy Mountain thrust in southern Nevada there was in increase in microfracture density in sandstones as the principal fault surface is approached. A similar observation was made around large strike-slip faults (Chester and Logan, 1986). This, as discussed earlier, was expected based on experimental observations where faults were preceded by coalescence of microcracks about the future failure plane (Scholz, 1968b; Lockner et al., 1991; Moore and Lockner, 1995). Microfracture-density field studies show that, for some faults, microfractures exhibit an exponential increase as the principal fault plan is approached (Wiltschko and Anders, 1994; Vermilye and Scholz, 1998; Mitchell and Faulkner, 2009; Faulkner et al., 2011; Mitchell and Faulkner, 2012; Mizoguchi and Ueta, 2013). Fig. 2d shows a sample from the damage zone of a Tertiary granite sampled 300 m from the principal fault surface of a normal

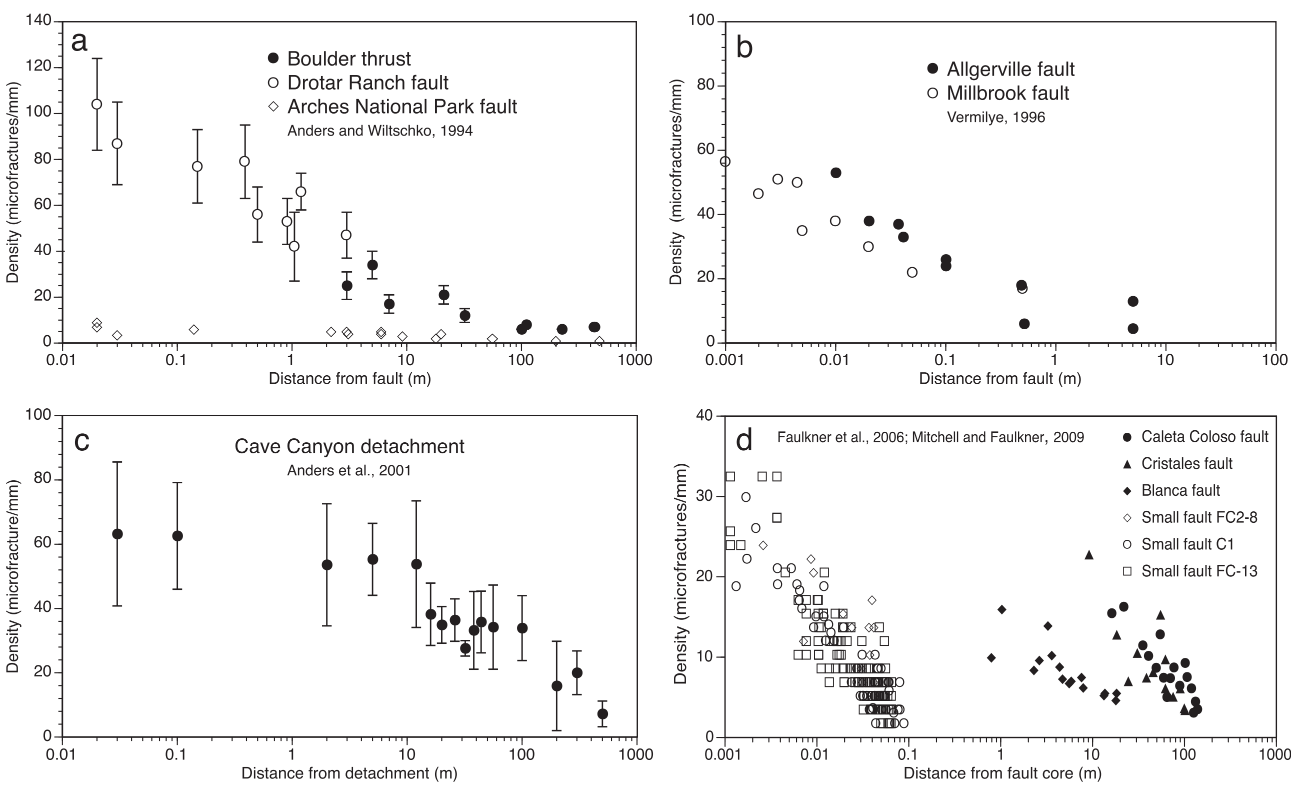

Fig. 4. Microfracture density as a function of distance from several faults of various displacement. See Anders et al. (2013) for details of sampling locations. (a) Microfracture density in sandstones, arkoses, and quartzites, from Anders and Wiltschko (1994), (b) microfracture density in quartzites, from Vermilye (1996). (c) Microfracture density in a Tertiary granite, from Anders et al. (2001). (d) Microfracture density in granodiorites, from Faulkner et al. (2006) and Mitchell and Faulkner (2009).

Please cite this article in press as: Anders, M.H., et al., Microfractures: A review, Journal of Structural Geology (2014), http://dx.doi.org/10.1016/j.jsg.2014.05.011

fault with a displacement of 5 km, and Fig. 2e shows a sample from the transition between the damage zone and fault core taken 12 m from the principal fault surface of the same fault. As shown in Fig. 4, numerous studies have demonstrated an exponential relationship in microfracture density and fault-surface proximity. At a given distance, depending on rock type and ambient stresses, there is a fall-off of this relationship to a background level of density (Anders et al., 2013).

4.5. Microfracture orientation patterns in fault damage zones

Brittle fracturing in quartz exhibits no strongly preferred orientation (Tuttle, 1949), making quartz a good medium for assessment of the orientation of applied stresses. However, c-axis indenter studies of quartz indicate that some anisotropy exists (Timms et al., 2010), although it is unclear how pronounced the anisotropy is under tectonic deviatoric stress conditions. Quartz composes sedimentary rocks such as sandstones, arkoses, and conglomerates, as well as igneous rocks and metamorphic rocks. Because microfractures are, as mentioned above, Mode I fractures, they have been shown by numerous authors to provide important information about the paleostress orientations in many natural settings (Tuttle, 1949; Wise, 1964; Friedman, 1969; Engelder, 1974; Brock and Engelder, 1977; Knipe and White, 1979; Dula, 1981; Anders, 1982; Lespinasse and Pêcher, 1986; Kowallis et al., 1987; Laubach, 1988a,1989,1997; Fleischmann, 1990; Blenkinsop, 1990; Onasch, 1990; Wang and Sun, 1990; Anders and Wiltschko, 1994; Vermilye and Scholz, 1998; Boullier, 1999; Wilson et al., 2003; Gomez and Laubach, 2006; Laubach and Ward, 2006; Laubach and Diaz-Tushman, 2009; Mitchell and Faulkner, 2009, 2012; Anders et al., 2013; Mizoguchi and Ueta, 2013). Microfractures also proved useful for testing fold-fracture models (Narahara and Wiltschko, 1986; Laubach, 1988a, Ismat and Mitra 2005; Ismat, 2008; Iñigo et al., 2012). Moreover, much can be inferred from relatively sparse sampling of regional patterns or local fault-zone patterns from small samples taken from drilling core or cuttings (e.g., Kowallis et al., 1987; Blenkinsop, 1990; Wang and Sun, 1990; Anders and Christie-Blick, 1994; Martin and Bergerat, 1996; Laubach and Gale, 2006; Hooker et al., 2009).

Sedimentary rocks that are weakly lithified tend to transfer stresses at points of grain contact (e.g., Borg and Maxwell, 1956; Friedman, 1963; Engelder, 1974; Brock and Engelder, 1977; Knipe and White, 1979; Anders, 1982; Anders and Wiltschko, 1994; Shipton and Cowie, 2001). Microfractures that radiate from a point source (Fig. 2f) require large numbers of measurements in order to overcome the statistical dispersion created by this pattern. Moreover, sampling large populations of microfracture orientations in siliciclastic sedimentary rocks is also necessary because these rocks commonly have grains that contain inherited microfractures (e.g., Sipple, 1968; Anders et al., 2013; Fig. 1h). Examples of this include the study by Wilson et al. (2003), who measured over 8000 microfracture orientations in sandstones in order to assess paleostress orientations surrounding the Punchbowl fault, an inactive branch of the San Andreas fault (Fig. 5a). Similarly, Anders and Wiltschko (1994) measured a total of over 8000 microfracture orientations in arenites surrounding normal and thrust faults (Fig. 5b). Both Anders and Wiltschko (1994) and Vermilye and Scholz (1998) used microfracture orientations surrounding a fault to demonstrate that fractures on opposite sides of a fault yield different orientations depending on slip direction (Figs. 5b and 6). Orientation data from a small displacement fault (Fig. 6) as well as the larger ones of Anders and Wiltschko (1994) were found to be consistent with a process-zone fracture aureole around a fault tip. As discussed in the last section, all studies of microfracture orientations near fault surfaces present the possibility that some of the microfractures arise as a result of fault waviness or are inherited from older events (Wilson et al., 2003; Faulkner et al., 2011). However, as we have discussed, CL can be used to mediate this inheritance problem by identifying crosscutting relationships.

5. Microfractures and macrofractures

In addition to fluid-inclusion planes associated with localized folds and faults, there are commonly strong regionally developed preferred orientations. Many studies demonstrate a parallelism between the orientation of microfractures and larger macrofractures (Tuttle, 1949; Riley, 1947; Bonham, 1957; Wise, 1964; Roberts, 1965; Harper, 1966; Friedman, 1969; Dula, 1981; Laubach, 1989; Vermilye and Scholz, 1998; Laubach and Diaz-Tushman, 2009). As discussed in Section 3, microfractures nucleate at stress concentrations that occur at the grain scale. Once microfractures become longer than that length scale, i.e., become transgranular, they may continue to propagate by virtue of the stress concentration at the tip and become macrofractures. Such microfractures share common orientations with macrofractures of the same set (Laubach, 1989) and they may belong to a common, systematic size distribution (e.g., Hooker et al., 2009). Mode I cracks grown in the laboratory are observed to form a process zone of grain-scale

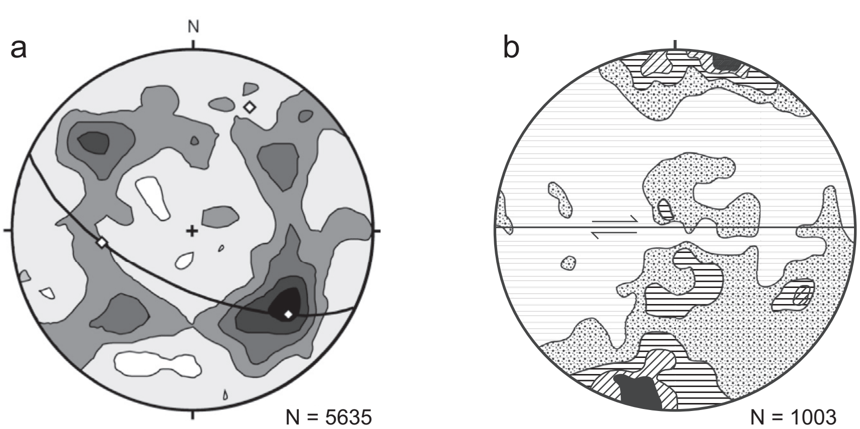

Fig. 5. Plots of poles to microfracture on stereonet projections. (a) Poles to microfracture FIPs from a sandstone sampled in the damage zone of the Punchbowl fault of Southern California (represents a subset of the total measurements from Wilson et al., 2003). Great circle represents the fault surface and diamonds represent the normal to the fault surface, slip direction (SW quadrant) and *b*-axis. (b) Poles to microfractures from samples collected in proximity of the Boulder thrust of the Lyon Sandstone. Equatorial line represents the fault surface and arrows the movement directions (represents a subset of the total measurements from Anders and Wiltschko, 1994).

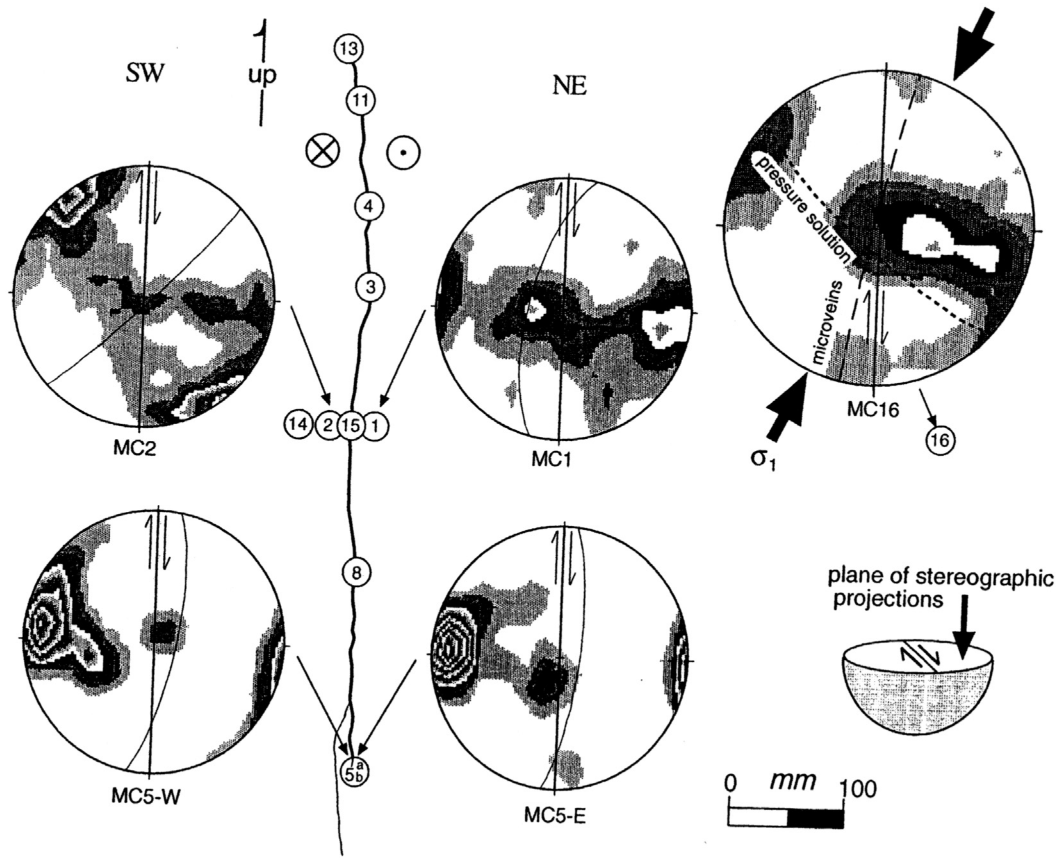

Fig. 6. Orientation of microfractures surrounding a small displacement strike-slip Millbrook Cliff fault. The fault is in Silurian-age Shawnangunk Formation quartzites of the Shawnangunk Mountains of southern New York (from Vermilye and Scholz, 1998).

microfractures (Swanson, 1987; Labuz et al., 1987). As the master crack grows, the microfractures in the process zone are left behind and become inactive, forming what is known as the damage zone. The width of the crack-tip stress concentration scales with the length of the master crack, so the process zone width grows in concert with the growth of the master crack. The damage zones surrounding some joints and dikes are often highlighted by mineralized halos, making them readily recognizable (Engvik et al., 2005, 2009). Fig. 7 shows approximately linear scaling between damage-zone width and the aperture of joints and dikes. The crack-tip stress field of a Mode I crack is dominated by tensile stresses normal to the plane of the crack. Hence microfractures in the process zones of joints and dikes will tend to have orientations parallel to those structures. For example, Delaney et al. (1986) found clusters of subparallel joints surrounding dikes. Some of the clustering of microfractures observed in scan lines may be damage zones surrounding macrofractures.

Populations of fractures having a diverse range of fracture sizes may arise from the evolution of some microfractures into macrofractures within an overall disseminated population of fractures, or the correlation could result from microfractures created by crack-tip stress concentrations in a process zone near a growing fracture of larger size (Atkinson, 1987). Although not mutually exclusive, the relative importance of these two processes – growth of select disseminated fractures and byproducts of process zones – has yet to be rigorously explored with observational studies, yet fluid-inclusion analysis may permit such tests in some cases (Hooker et al., 2012b).

Many early workers on fluid-inclusion planes noticed that these microstructures shared common orientations with arrays of larger fractures. Subsequent work combining CL imaging and fluid-inclusion analysis has demonstrated that many quartz-filled microfractures share mineral assemblages, CL textures and colors, crosscutting relations, and other attributes that suggest that the small fractures are merely the small-size fractions of larger fractures (Laubach, 1989; Fig. 2b and c). Where microfractures are parts

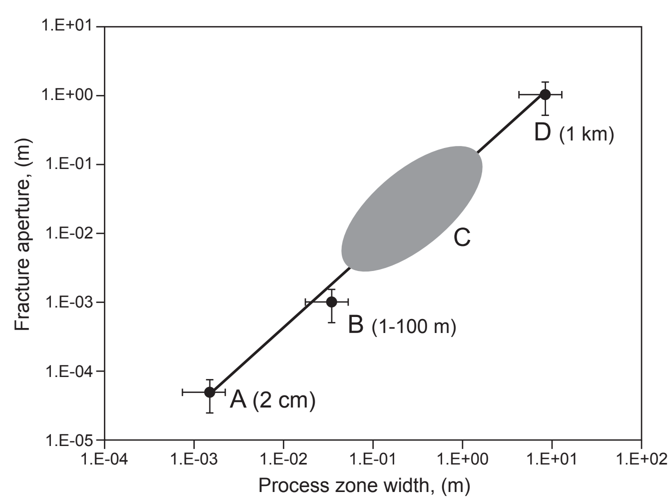

Fig. 7. A log–log plot of process zone width versus aperture of joints and dikes. Fracture length given in brackets. Data sources: (A) lab experiments on opening mode cracks in granite (Swanson, 1987), (B) joints in granite (Segall, 1984; Segall and Pollard, 1980). (C) Dikes in gneisses (Engvik et al., 2005), and (D) dikes in sandstone (Delaney et al., 1986). From Scholz (2011).

of fracture populations that include large fractures, microfractures can be used as proxies for large fractures in cases where more numerous microfractures are readily sampled, for example in subsurface studies where fracture abundance may vary (Fig. 8). Combination of CL and fluid-inclusion studies allows this timing relationship to be quantified, and permits reconstruction of the growth of fractures from microfractures (Becker et al., 2010; Fall et al., 2012). Results of this early work suggest that such assemblages record complex fracture-array growth histories – good news for future fracture studies, which too frequently are beset by end products (fracture geometry and patterns) that might have arisen from several loading paths.

6. Microstructures that resemble microfractures

Deformation lamellae (Fig. 1g) and shock lamellae (Fig. 9) often can be confused with Mode I microfractures, especially when the lamellae exhibit an optically visible track of fluid inclusions. These kinds of planar deformation features (PDFs), as found in quartz, are features associated with limited displacement along crystallographic planes, unlike Mode I microfractures, the orientations of which are a direct response to local deviatoric stresses. Commonly deformation lamellae are found in metamorphic rocks and associated with features like undulose extinction (e.g., Christie and Raleigh, 1959; McLaren and Hobbs, 1972; Blenkinsop and Drury, 1988). Although less common, PDFs can also be found in minerals deformed in the brittle field or in igneous bodies where differential cooling can create high intergranular stresses (e.g., Drury, 1993; Anders et al., 2001). Böhm lamellae (Böhm, 1883; Groshong, 1988), in the broadest sense, are deformation lamellae, typically with fluid-inclusion planes that are visible using an optical microscope. Although deformation and shock lamellae both can have fluid inclusions along the lamellae, these inclusions typically cannot be recognized with the magnification of a SEM. Experimental studies have shown that deformation lamellae form by dislocations involving glide and climb-control, occurring most commonly near or along the basal {0001} plane in quartz (Vernooij and Langenhorst, 2005), similar to Dauphine twins (Wenk et al., 2006). Deformation lamellae are often manifesting as roughly parallel curviplanar surfaces that are seen, on close inspection, as a series of anastomosing dislocation surfaces (Vernooij and Langenhorst, 2005; Fig. 1g). Shocked quartz, on the other hand, forms as sharp distinct lamellae along crystallographic planes, often exhibiting multiple planar sets (Fig. 8; Leroux et al., 1994; Grieve et al., 1996). The lamellae in shocked quartz are thin planes of glass formed along crystallographic planes (Gratz et al., 1996). Annealing can result in precipitation of extremely small water bubbles in the lamellae (Grieve et al., 1996; Langenhorst and Deutsch, 1998) not visible optically. For a further discussion of techniques to distinguish between PDFs and Mode I microfractures, see French and Koeberl (2010).

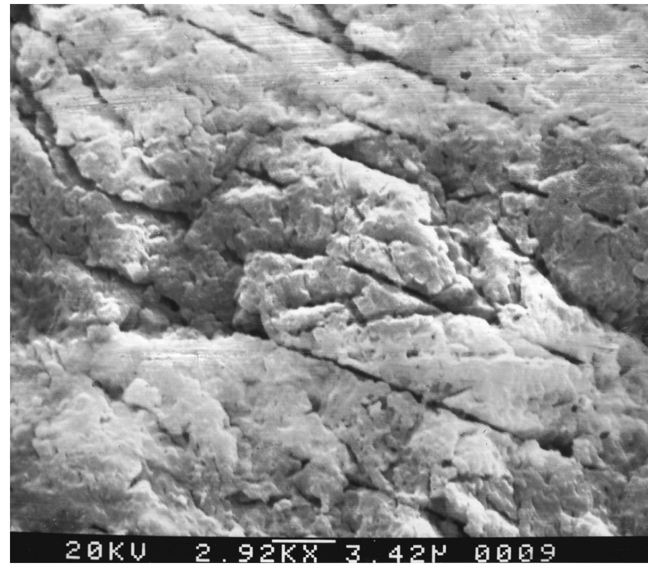

Fig. 9. SEM image of shocked quartz from the Cretaceous/Tertiary boundary from Raton Pass in southern Colorado. Sampled was etched in HF to accentuate the lamellae. One strong preferred orientation of lamellae and two weakly expressed lamellae are discernable in this image. Scale bar is 3.42 µm.

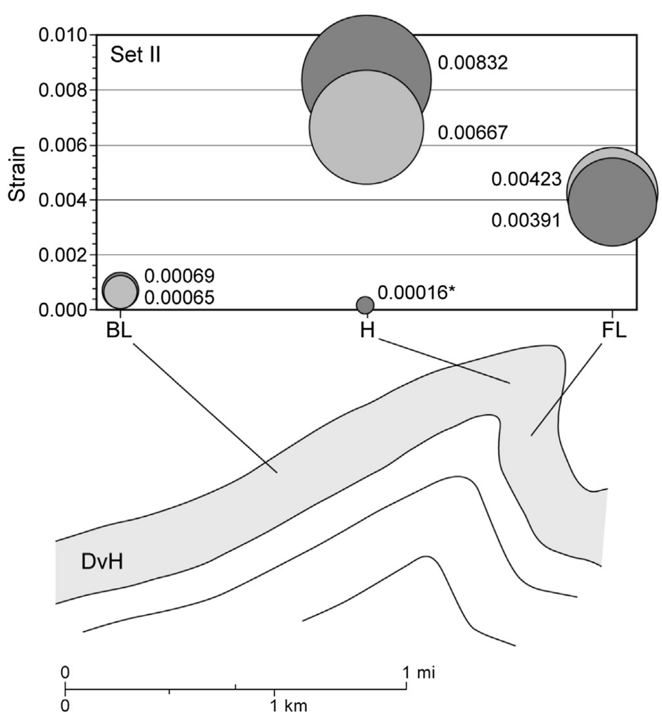

Fig. 8. Microfracture strain versus fold geometry. This example illustrates the use of microfractures to document strain and microfracture abundance variation with structural position. Strain measurements are derived from microfracture kinematic aperture scan lines. In this example, microfracture abundance was used as a proxy for macrofracture abundance because of sparse core observations of large fractures. The diagram also compares subsurface core and outcrop data. The asterisk symbol (*) indicates an outcrop sample. Here outcrop microfractures are less abundant than those of the same Set II microfractures in the subsurface, suggesting that these outcrops do not contain optimal analogs for subsurface structures. Example from Devonian Huamampampa Formation (DvH), Subandean ranges fold and thrust belt, fracture set II, Bolivia. Circle size is linearly proportional to fracture strain. BL, back limb; H, hinge; and FL, forelimb. From Iñigo et al. (2012).

7. Practical use of microfractures

Sampling of fractures that may be more widely spaced than dimensions of the accessible rock volume is a challenge for systematic fracture assessment in subsurface rocks (Narr, 1991; Ortega et al., 2006). The problem is acute in flat-lying to gently dipping sedimentary rocks, where cores cut at high angles to steeply dipping fractures may miss cm- to meter-length fractures that have spacing of tens of centimeters to many meters or more (Gale, 2002; Hooker et al., 2009). Such widely spaced fractures cannot be sampled systematically by 20-cm-diameter vertical well bores or 10-cm-diameter cores; a consequence is lack of consistent data on fracture orientation and abundance, making it harder to test models that predict subsurface fracture occurrence – to the detriment of efficient fracture assessment in deep, fractured rocks.

If microfractures are part of a population that includes large fractures, microfracture analysis is one way to overcome sparse observations of large fractures. Microfractures are useful because, in many sandstones and in some other rocks, microfractures are more abundant than associated macrofractures (Laubach, 1989; Hooker et al., 2014). Individual transgranular microfractures can be used to determine fracture strike (Laubach, 1997) and microfracture size populations can be used to assess fracture abundance (Marrett et al., 1999; Ortega and Marrett, 2000; Hooker et al., 2009; Iñigo et al., 2012). Because they may also be sealed with cement, these structures are inconspicuous unless sought using sensitive imaging methods such as cathodoluminescence (CL). Nevertheless sealed microfractures may provide information about larger fractures that are open because small fractures, with their small volume relative to surface area, seal more readily than wider fractures (Laubach, 2003). If suitable microfractures are present, they can be used to evaluate the number and orientation of fracture sets and, using inexpensive wire line sampling methods, to estimate fracture abundance and quantify fracture-size distribution, even in small volumes of rock (Laubach and Gale, 2006) (Fig. 8). Microfracture populations can also be used to distinguish between landslide detachments and detachments that are tectonic in origin (Anders et al., 2010; 2013). This distinction can be further advanced by CL techniques where identification of crosscutting relationships found ina microfracture population can establish a movement history.

Another practical use of microfracture studies is to inform further development of predictive geomechanical and geostatistical models. For example, to simulate the growth of fracture patterns, many current geomechanical models are seeded with microfractures, but these are usually introduced at the outset of experiments, are large and uniform, and do not have attributes that evolve with thermal history (and few geomechanical models account for thermal history; Olson et al., 2009, describe an exception). These attributes are unlike natural microfractures, which, as we have seen, may be absent or very sparse in some rocks (Gale et al., 2014) and span a size range of several orders of magnitude (Marrett et al., 1999; Hooker et al., 2014), and may form during protracted deformation (Hooker et al., 2012a). In many rocks, microfractures are ephemeral mechanical features owing to cement deposition and creep. This pattern is particularly evident in quartz-rich rocks (Laubach, 2003; Laubach and Diaz-Tushman, 2009) and dolostones (Gale et al., 2010) in which microfracture pore space is systematically destroyed by exposure to high temperatures. Should microfractures be introduced into geomechanical models in different amounts and patterns depending on rock type and thermal history? Will such changes make a difference in the final fracture pattern? Microfracture closure – the way microfractures either become fossilized by sealing processes or grow to larger sizes – is an area where progress has been impeded by boundaries based on observation technique (TL versus CL), and by a narrow focus on specific rock types. Issues such as the evolution of fracture porosity with thermal history, the mechanical effects of the cement itself (if any) and how size scaling arises (Hooker et al., 2012a; 2013) are topics where new experiments and theoretical approaches could be fruitful.

8. Conclusions and speculation on future research directions

From the first time they were recognized by naturalists using optical microscopes, the importance of microfractures as a geological tool has grown. Advances in the 1960s led to an understanding of the critical function of Mode I microfractures in the initiation of faults. This work showed how, in experimental settings, even the smallest faults in brittle rock are preceded by a cloud of Mode I microfractures just prior to failure (Brace et al., 1966; Scholz, 1968a; Lockner et al., 1991; Reches and Lockner, 1994; Moore and Lockner, 1995). In the 1960s and 1970s,advances were made using TL technique to assess paleostress orientations (Wise, 1964; Friedman, 1969; Engelder, 1974; Brock and Engelder, 1977). Later these techniques played a critical role in developing theories about how natural faults grow in a process zone from small faults to larger fault systems (Scholz et al., 1993; Anders and Wiltschko, 1994; Wilson et al., 2003; Mitchell and Faulkner, 2009). In many rocks, microfractures are filled by cement deposits, a characteristic particularly evident in quartz-rich rocks and some carbonates (Laubach, 2003; Gale et al., 2010) where microfracture pore space is cement in optical continuity with host rock. Recent advances in microscopy such as SEM, TEM, and CL allow identification of microfractures in a greater range of rocks and the ability to define complex history, including: (1) the character of fluids residing in or moving through the rock (Pêcher et al., 1985; Lespinasse, 1999; Fall et al., 2012); (2) microfracture porosity as a function of thermal history; (3) relative timing from crosscutting relationships. As we have discussed, advances may come from more interaction between researchers focused on natural microfractures, those studying arrays of larger macrofracture networks, and the fluid-inclusion and geochemistry communities, particularly because a combination of these approaches can help unravel the timing and rates of growth of individual fractures and fracture populations. The tendency for students of microfractures to focus on specific rock types, notably quartz-rich sandstones, quartzites, and granite, may have been an impediment to progress; universal structural and geochemical processes may vary in informative ways among these different host rock types. Microfracture growth in reactive environments is an area where new experiments, theoretical approaches, and field observations could be fruitful.

Acknowledgments

The authors would like to recognize the contributions, intellectual and otherwise, of David V. Wiltschko to our understanding of the importance of microfracturing. Dave was the thesis advisor for MHA while both were at the University of Michigan. We will miss him as a scientist but mostly as a friend. We thank Rick Groshong, Charlie Onasch, and Tom Blenkinsop for helpful reviews and Chris Parker for editorial comments. We would also like to thank Maureen M. Anders for help with the graphics. SEL's work is funded partly by grant DE-FG02-03ER15430 from Chemical Sciences, Geosciences and Biosciences Division, Office of Basic Energy Sciences, Office of Science, U.S. Department of Energy and by the Fracture Research and Application Consortium.

References

Microfractures: theory

Atkinson, B.K., 1987. Introduction to fracture mechanics and its geophysical applications. In: Atkinson, B.K. (Ed.), Fracture Mechanics of Rock. Academic Press, London, pp. 1–26.
Clark, M.B., Brantley, S.L., Fisher, D.M., 1995. Power-law vein-thickness distributions and positive feedback in vein growth. Geology 23 (11), 975–978.
Cowie, P.A., Scholz, C.H., 1992. Displacement-length scaling relationship for faults: data synthesis and discussion. J. Struct. Geol. 14 (10), 1149–1156.
Griffith, A.A., 1920. VI. The phenomena of rupture and flow in solids. Phil. Trans. R. Soc. Lond. A 221, 163–198.
Healy, D., Jones, R.R., Holdsworth, R.E., 2006a. New insights into the development of brittle shear fractures from a 3D numerical model of microcrack interaction. Earth Planet. Sci. Lett. 249, 14–28.
Healy, D., Jones, R.R., Holdsworth, R.E., 2006b. Three-dimensional brittle shear fracturing by tensile crack interaction. Nature 439, 64–67.

Hoagland, R.G., Hahn, G.T., Rosenfield, A.R., 1973. Influence of microstructure in fracture propagation in rock. Rock Mech. 5, 77–106.

Hooker, J.N., Eichhubl, P., Laubach, S.E., 2012b. Reconstructing the growth of a fracture set using fluid inclusion microthermometry, El Alamar Formation (Triassic), NE Mexico (abs.). In: AGU Fall Meeting, Abstract T21A-2556.

Hooker, J.N., Gale, J.F.W., Gomez, L.A., Laubach, S.E., Marrett, R., Reed, R.M., 2009. Aperture-size scaling variations in a low-strain opening-mode fracture set, Cozzette Sandstone, Colorado. J. Struct. Geol. 31, 707–718.

Hooker, J.N., Gomez, L.A., Laubach, S.E., Gale, J.F.W., Marrett, R., 2012a. Effects of diagenesis (cement precipitation) during fracture opening on fracture aperture-size scaling in carbonate rocks. In: Garland, J., Neilson, J.E., Laubach, S.E., Whidden, K.J. (Eds.), Advances in Carbonate Exploration and Reservoir Analysis, Geological Society of London, Special Publication, vol. 370, pp. 187–206. http://dx.doi.org/10.1144/SP370.9.

Hooker, J.N., Laubach, S.E., Gomez, L.A., Marrett, R., Eichhubl, P., Diaz-Tushman, K., Pinzon, E., 2011. Fracture size, frequency, and strain in the Cambrian Eriboll Formation sandstones, NW Scotland. Scottish J. Geol. 47, 45–56.

Hooker, J.N., Laubach, S.E., Marrett, R., 2013. Fracture-aperture size – frequency, spatial distribution, and growth processes in strata-bounded and non-strata-bounded fractures, Cambrian Mesón Group, NW Argentina. J. Struct. Geol. 54, 54–71.

Hooker, J.N., Laubach, S.E., Marrett, R., 2014. A universal power-law scaling exponent for fracture apertures in sandstone. Geol. Soc. Am. Bull. http://dx.doi.org/10.1130/B30945.1.

Horii, H., Nemat-Nasser, S., 1985. Commpression-induced microcrack growth in brittle solids: axial splitting and shear failure. J. Geophys. Res. 90 (B), 3105–3125.

Irwin, G.R., 1958. Fracture. In: Flugge, S. (Ed.), Handbuch der Physik. Springer-Verlag, Berlin, pp. 551–590.

Kranz, R.L., 1983. Microcracks in rocks: a review. Tectonophysics 100, 449–480.

Loriga, M.A., 1999. Scaling systematics of vein size: an example from the Guanajuato mining district (central Mexico). Geol. Soc. London Spec. Pub. 155, 57–67.

Marrett, R., 1996. Aggregate properties of fracture populations. J. Struct. Geol. 18 (2/3), 169–178.

Marrett, R., Ortega, O.J., Kelsey, C.M., 1999. Extent of power-law scaling for natural fractures in rock. Geology 27 (9), 799–802.

Narr, W., 1991. Fracture density in the deep subsurface: techniques with application to Point Arguello oil field. AAPG Bull. 75 (8), 1300–1323.

Olson, J.E., 2003. Sublinear scaling of fracture aperture versus length: an exception of the rule? J. Geophys. Res. 108 (B9), 2413 http://dx.doi.org/10.1029/2001JB000419.

Olson, J.E., Schultz, R.A., 2011. Comments on "a note on the scaling relations for opening mode fractures in rock" by Scholz, C.H. J. Struct. Geol. 33 (10), 1523–1524.

Ortega, O.J., Marrett, R., Laubach, S.E., 2006. A scale-independent approach to fracture intensity and average spacing measurement. AAPG Bull. 90 (2), 193–208.

Pollard, D.D., Segall, P., Selaney, P.T., 1982. Formation and interpretation of dilatant echelon cracks. Geol. Soc. Am. Bull. 93 (12), 1291–1303.

Schlische, R.W., Young, S.S., Ackermann, R.V., Gupta, A., 1996. Geometry and scaling relations of a population of very small rift-related normal faults. Geology 24 (8), 683–686.

Scholz, C.H., 1995. Fractal transitions on geological surfaces. In: Barton, C.A., LaPointe, P.R. (Eds.), Fractals in the Earth Sciences. Plenum Press, New York.

Scholz, C.H., 2002. The mechanics of earthquakes and faulting. Cambridge University Press, Cambridge, p. 471.

Scholz, C.H., 2010. A note on the scaling relations for opening mode fractures in rock. J. Struct. Geol. 32, 1485–1487.

Scholz, C.H., 2011. Reply to Jon Olson and Richard Schultz. J. Struct. Geol. 33, 1525–1526.

Scholz, C.H., Hickman, S.H., 1983. Hysteresis in the closure of a nominally flat crack. J. Geophys. Res. 88, 6501–6504.

Scholz, C.H., Dawers, N.H., Yu, J., Anders, M.H., Cowie, P.A., 1993. Fault growth and fault-scaling laws: preliminary results. J. Geophys. Res. 98 (B12), 21951–21961.

Schultz, R.A., Klimczak, C., Fossen, H., Olson, J.E., Exner, U., Reeves, D.M., Soliva, R., 2013. Statistical tests of scaling relationships for geologic structure. J. Struct. Geol. 48, 85–94.

Schultz, R.A., Soliva, R., Fossen, H., Okubo, C.H., Reeves, D.M., 2008. Dependence of displacement–length scaling relations for fractures anddeformation bands on the volumetric changes across them. J. Struct. Geol. 30, 1405–1411.

Segall, P., 1984. Formation and growth of extensional fracture sets. Geol. Soc. Am. Bull. 95, 454–462.

Simmons, G., Richter, D., 1976. Microcracks in rocks. In: Strens, R.G.J. (Ed.), The Physics and Chemistry of Minerals and Rocks. Interscience, New York, pp. 105–137.

Simmons, G., Todd, T., Baldridge, W.S., 1975. Toward a quantitative relationship between elastic properties and cracks in low porosity rocks. Am. J. Sci. 275, 318–345.

Sorby, H.C., 1858. On the microscopic structure of crystals, indicating the origin of minerals and rocks. Geol. Soc. Lond. Q. J. 14, 453–500.

Snow, D.T., 1970. The frequency and apertures of fractures in rock. Int. J. Rock Mech. Mining Sci. 7, 23–40.

Spyropoulos, C., Scholz, C.H., Shaw, B.E., 1999. Transition regimes for growing crack populations. Phys. Rev. E. http://dx.doi.org/10.1103/PhysRevE.65.056105.

Vermilye, J.M., Scholz, C.H., 1995. Relation between vein length and aperture. J. Struct. Geol. 17 (3), 423–434.

Wang, C.-Y., Sun, Y., 1990. Orientation microfractures in Cajon Pass drill cores: stress field near the San Andreas fault. J. Geophys. Res. 95 (B7), 11,135–11142.

Wilson, J.E., Chester, J.S., Chester, F.M., 2003. Microfracture analysis of fault growth and wear processes, Punchbowl Fault, San Andreas system, California. J. Struct. Geol. 25/11, 1855–1873.

Wise, D.U., 2005. Rift and grain in basement thermally triggered snapshots of stress fields during erosional unroofing of the Rocky Mountains of Montana and Wyoming. Rocky Mountain Geol. 40 (2), 193–209 http://dx.doi.org/10.2113/40.2.193.

Microfractures: laboratory experiments

Barnhoorn, A., Cox, S.F., Robinson, D.J., Senden, T., 2010. Geology 38 (9), 779–782.

Borg, I.Y., Friedman, M., Handin, J., Higgs, D.V., 1960. Experimental deformation of St. Peter Sand: a study of cataclastic flow. In: Griggs, D., Handin, J. (Eds.), Rock Deformation, GSA Memoirs, vol. 79, pp. 133–192 (Chapter 6).

Borg, I.Y., Maxwell, J.C., 1956. Interpretations of fabrics of experimentally deformed sands. Am. J. Sci. 254, 71–81.

Brace, W.F., Orange, A.S., 1968. Electrical resistivity changes in saturated rocks during fracture and frictional sliding. J. Geophys. Res. 73 (4), 1433–1445.

Brace, W.F., Paulding, B.W., Scholz, C.H., 1966. Dilatancy in the fracture of crystalline rocks. J. Geophys. Res. 71, 3939–3953.

David, C., Wong, T.F., Zhu, W., Zhang, J., 1994. Laboratory measurement of compaction-induced permeability change in porous rocks: implications for the generation and maintenance of pore pressure excess in the crust. Pure Appl. Geophys. 143 (1-3), 425–456.

Friedman, M., 1963. Petrofabric analysis of experimentally deformed calcite-cemented sandstones. J. Geol. 71, 12–37.

Gallegher, J.J., Friedman, M., Handin, J., Sowers, G.M., 1974. Experimental studies relating to microfractures in sandstone. Tectonophysics 21, 203–243.

Gratz, A.J., Fisler, D.K., Bohor, B.F., 1996. Distinguishing shocked from tectonically deformed quartz by the use of the SEM and chemical etching. Earth Planet. Sci. Lett. 142 (3), 513–521.

Katz, O., Reches, Z., 2004. Microfracture, damage, and failure in brittle granites. J. Geophys. Res. 109, B01206 http://dx.doi.org/10.1029/2002JB001961.

Kranz, R.L., 1979. Crack growth and development during creep of Barre granite. Int. J. Rock Mech. Mining Sci. 16, 23–35.

Labuz, J.F., Shah, S.P., Dowding, C.H., 1987. The fracture process zone in granite – evidence and effect. Int. J. Rock Mech. Mining Sci. Geomech. Abstr. 24 (4), 235–246.

Lockner, D.A., Byerlee, J.D., Kuksenko, V., Ponomarev, A., Sidorin, A., 1991. Quasi-static fault growth and shear fracture energy in granite. Nature 350 (6313), 39–42.

Maxwell, J.C., 1960. Experiments on compaction and cementation of sand. In: GSA Memoir, 79, pp. 105–132.

Mogi, K., 1962. Study of elastic shocks caused by the fracture of heterogenous materials and their relation to earthquake phenomena. Bull. Earthquake Res. Inst. Univ. Tokyo 40, 125–173.

Mogi, K., 1971. Fracture and flow of rocks under high triaxial compression. J. Geophys. Res. 76, 1255.

Moore, D.E., Lockner, D.A., 1995. The role of microcracking in shear-fracture propagation in granite. J. Struct. Geol. 17 (1), 95–114.

Reches, Z., Lockner, D.A., 1994. Nucleation and growth of faults in brittle rocks. J. Geophys. Res. 99 (B9), 18159–18173.

Scholz, C.H., 1968a. Microfracturing and the inelastic deformation of rock in compression. J. Geophys. Res. 73, 1417–1432.

Scholz, C.H., 1968b. Experimental study of the fracturing processes in brittle rock. J. Geophys. Res. 73, 1447–1454.

Scholz, C.H., Koczynski, T.A., 1979. Dilatancy anisotropy and the response of rock to large cyclic loads. J. Geophys. Res. 84, 5525–5534.

Spyropoulos, C., Griffith, W.J., Scholz, C.H., Shaw, B.E., 1999. Experimental evidence for different strain regimes of crack populations in a clay model. Geophys. Res. Lett. 26 (8), 1081–1084.

Swanson, P.L., 1987. Tensile fracture resistance mechanisms in brittle polycrystals: an ultrasonics and in situ microscopy investigation. J. Geophys. Res. 92 (B8), 8015–8036.

Tapponnier, P., Brace, W.F., 1976. Development of stress-induced microcracks in Westerly granite. Int. J. Rock Mech. Mining Sci. 13, 103–112.

Tham, L.G., Liu, H., Tang, C.A., Lee, P.K.K., Tsui, Y., 2005. On tension failure of 2-D rock specimens and associated acoustic emission. Rock Mech. Rock Engin. 38, 1–19.

Timms, N.E., Healy, D., Reyes-Montes, J.M., Collins, D.S., Prior, D.J., Young, R.P., 2010. Effects of crystallographic anisotropy on fracture development and acoustic emission in quartz. J. Geophys. Res. 115, B07202 http://dx.doi.org/10.1029/2009JB006765.

Vernooij, M.G.C., Langenhorst, F., 2005. Experimental reproduction of tectonic deformation lamellae in quartz and comparison to shock-induced planar deformation features. Meteor. Planet. Sci. 40 (9–10), 1353–1361.

Wenk, H.R., Rybacki, E., Dresen, G., Lonardelli, I., Barton, N., Franz, H., Gonzalez, G., 2006. Dauphine twinning and texture memory in polycrystalline quartz. Part 1: experimental deformation of novaculite. Phys. Chem. Miner. 33 (10), 667–676.

Wong, T.-F., 1982. Micromechanics of faulting in Westerly granite. Int. J. Rock Mech. Mining Sci. 19, 49–64.

Please cite this article in press as: Anders, M.H., et al., Microfractures: A review, Journal of Structural Geology (2014), http://dx.doi.org/10.1016/j.jsg.2014.05.011

Wong, T.F., Szeto, H., Zhang, J.X., 1992. Effect of loading path and porosity on the failure mode of porous rocks. Appl. Mech. Rev. 45 (8), 281–293 http://dx.doi.org/10.1115/1.3119759.

Microfractures: faults, folds and paleostress

Anders, M.H., 1982. Nature of Microfracturing Around Naturally Occurring Faults. MS thesis. University of Michigan, Ann Arbor, Michigan, p. 34.
Anders, M.H., Christie-Blick, N., 1994. Is the Sevier Desert reflection of west-central Utah a normal fault? Geology 22, 771–774.
Anders, M.H., Fouke, B.W., Zerkle, A.L., Tavarnelli, E., Alvarez, W., Harlow, G.E., 2010. The role of calcining and basal fluidization in the long runout of carbonate slides: an example from the Heart Mountain slide block, Wyoming and Montana, U.S.A. J. Geol. 118, 577–599.
Anders, M.H., Schneider, J.R., Scholz, C.H., Losh, S., 2013. Mode I microfracturing and fluid flow in damage zones: the key to distinguishing faults from slides. J. Struct. Geol. 48, 113–125.
Anders, M.H., Wills, S., Christie-Blick, N., Krueger, S.W., 2001. Rock deformation studies in the Mineral Mountains and the Sevier Desert of west-central Utah: implications for upper crustal low-angle normal faulting. Geol. Soc. Am. Bull. 113, 895–907.
Anders, M.H., Wiltschko, D.V., 1994. Microfracturing, paleostress and the growth of faults. J. Struct. Geol. 16, 795–815.
Aviles, C.A., Scholz, C.H., Boatwright, J., 1987. Fractal analysis applied to characteristic segments of the San Andreas fault. J. Geophys. Res. 92 (B1), 331–344.
Barton, C.A., Zoback, M.D., 1992. Self-similar distribution of macroscopic fractures at depth in crystalline rock in the Cajon Pass scientific drill hole. J. Geophys. Res. 97 (B4), 5181–5200.
Blenkinsop, T.G., 1990. Correlation of paleotectonic fracture and microfracture orientations in cores with seismic anisotropy at Cajon Pass drill hole, southern California. J. Geophys. Res. 95 (B7), 11,143–11,150.
Blenkinsop, T.G., Drury, M.R., 1988. Stress estimates and fault history from quartz microstructures. J. Struct. Geol. 10 (7), 673–684.
Bonham, L.C., 1957. Structural petrology of the Pico anticline, Los Angeles County, California. J. Sediment. Petrol. 27, 251–264.
Bouchez, J.L., Delas, C., Gleizes, G., Nédélec, A., Cuney, M., 1992. Submagmatic microfractures in granites. Geology 20 (1), 35–38.
Brock, W.G., Engelder, T., 1977. Deformation associated with the movement of the Muddy Mountain overthrust in the Buffington window, southeastern Nevada. Geol. Soc. Am. Bull. 88, 1667–1677.
Chester, F.M., Chester, J.S., 2000. Stress and deformation along wavy frictional faults. J. Geophys. Res. 105 (B10), 23421–23430.
Chester, F.M., Logan, J.M., 1986. Implications for mechanical properties of brittle faults from observations of the Punchbowl fault zone, California. Pure Appl. Geophys. 124 (1–2), 79–106.
Dawers, N.H., Anders, M.H., Scholz, C.H., 1993. Growth of normal faults: displacement-length scaling. Geology 21, 1107–1110.
Dezayes, C.T., Villemin, T., Pêcher, A., 2000. Microfracture pattern compared to core-scale fractures in the borehole of the Soultz-sous-Forets granite, Rhine graben, France. J. Struct. Geol. 22, 723–733.
Dula Jr., W.F., 1981. Correlation between deformation lamellae, microfractures, macrofractures, and in situ stress measurements, White River Uplift, Colorado. Geol. Soc. Am. Bull. 92, 37–46. Plate 1.
Engelder, J.T., 1974. Cataclasis and the generation of fault gouge. Geol. Soc. Am. Bull. 85 (10), 1515–1522.
Faulkner, D.R., Mitchell, T.M., Healy, D., Heap, M.J., 2006. Slip on "weak" faults by the rotation of regional stress in the fracture damage zone. Nature 444, 922–925.
Faulkner, D.R., Mitchell, T.M., Jensen, E., Cembrano, J., 2011. Scaling of fault damage zones with displacement and the implications for fault growth processes. J. Geophys. Res. 116, B05403 http://dx.doi.org/10.1029/2010JB007788.
Fisher, Q.J., Knipe, R.J., 1998. Fault sealing processes in siliciclastic sediments. In: Geological Society of London, Special Publication, vol. 147, pp. 117–134 http://dx.doi.org/10.1144/GSL.SP.147.01.08.
French, B.M., Koeberl, C., 2010. The convincing identification of terrestrial meteorite impact structures: what works, what doesn't, and why. Earth-Sci. Rev. 98 (1), 123–170.
Friedman, M., 1969. Structural analysis of fractures in cores from Saticoy Field, Ventura County, California. AAPG Bull. 53, 367–389.
Grieve, R.A.F., Langenhorst, F., Stöffler, D., 1996. Shock metamorphism of quartz in nature and experiment: II. Significance in geoscience. Meteor. Planet. Sci. 31 (1), 6–35.
Gross, M.R., Engelder, T., 1995. Strain accommodated by brittle failure in adjacent units of the Monterey Formation, U.S.A.: scale effects and evidence for uniform displacement boundary conditions. J. Struct. Geol. 17 (9), 1303–1318.
Gudmundsson, A., 1987. Geometry, formation, and development of tectonic fractures on the Reykjanes Peninsula, southwest Iceland. Tectonophysics 139, 295–308.
Gupta, A., Scholz, C.H., 2000. Brittle strain regime transition in the Afar depression: implications for fault growth and seafloor spreading. Geology 28, 1087–1090.
Hancock, P.L., 1985. Brittle microtectonics: principles and practice. J. Struct. Geol. 7, 437–457.
Hicks, H., 1884. On the Cambrian conglomerates resting upon and in the vicinity of some pre-Cambrian rocks (the so-called intrusive masses) in Anglesey and Caernarvonshire. Geol. Soc. Lond. Q. J. 40, 187–199.
Homand, F., Hoxha, D., Belem, T., Pons, M.-N., Hoteit, N., 2000. Geometric analysis of damaged microcracks in granite. Mech. Mater. 32, 361–376.
Iñigo, J.F., Laubach, S.E., Hooker, J.N., 2012. Fracture abundance and patterns in the Subandean fold and thrust belt, Devonian Huamampampa Formation petroleum reservoirs and outcrops, Argentina and Bolivia. Mar. Petrol. Geol. 35, 201–218.
Ismat, Z., 2008. Folding kinematics expressed in fracture patterns: an example from the anti-Atlas fold belt, Morocco. J. Struct. Geol. 30 (11), 1396–1404 http://dx.doi.org/10.1016/j.jsg.2008.07.010.
Ismat, Z., Mitra, G., 2005. Folding by cataclastic flow: evolution of controlling factors during deformation. J. Struct. Geol. 27 (12), 2181–2203 http://dx.doi.org/10.1016/j.jsg.2005.08.005.
Jang, B.A., Wang, H.F., Ren, X., Kowallis, B., 1989. Precambrian paleostress from microcracks and fluid inclusions in the Wolf River batholith of Central Wisconsin. Geol. Soc. Am. Bull. 101, 1457–1464.
Kanaori, Y., 1986. A SEM cathodoluminescence study of quartz in mildly deformed granite from the region of the Atotsugawa fault, central Japan. Tectonophysics 131, 133–146.
Kanaori, Y., Yairi, K., Ishida, T., 1991. Grain boundary microcracking of granitic rocks from the northeastern region of the Atotsugawa fault, central Japan: SEM backscattered electron images. Eng. Geol. 30, 221–235.
Knipe, R.J., Lloyd, G.E., 1994. Microstructural analysis of faulting in quartzite, Assynt, NW Scotland: implications for fault zone evolution. Pure Appl. Geophys. 142, 229–254.
Knipe, R.J., White, S.H., 1979. Deformation in low grade shear zones in the Old Red Sandstone, S.W. Wales. J. Struct. Geol. 1, 53–66.
Kowallis, B.J., Wang, H.F., Jang, B.-A., 1987. Healed microcrack orientations in granite from Illinois borehole UPH-3 and their relationship to the rock's stress history. Tectonophysics 135, 297–306.
Langenhorst, F., Deutsch, A., 1998. Minerals in terrestrial impact structures and their characteristic features. In: Marfunin, A.S. (Ed.), Advanced Mineralogy, vol. 3. Springer, Berlin, pp. 95–119.
Laubach, S.E., Diaz-Tushman, K., 2009. Laurentian paleostress trajectories and ephemeral fracture permeability, Cambrian Eriboll Formation sandstones west of the Moine thrust zone, northwest Scotland. J. Geol. Soc. Lond. 166 (2), 349–362.
Laubach, S.E., Gale, J.F.W., 2006. Obtaining fracture information for low-permeability (tight) gas sandstones from sidewall cores. J. Petrol. Geol. 29 (2), 147–158.
Laubach, S.E., Olson, J.E., Gale, J.F.W., 2004b. Are open fractures necessarily aligned with maximum horizontal stress? Earth Planet. Sci. Lett. 222 (1), 191–195.
Laubach, S.E., Olson, J.E., Gross, M.R., 2009. Mechanical and fracture stratigraphy. AAPG Bull. 93, 1413–1426.
Lespinasse, M., Cathelineau, M., 1995. Paleostress magnitudes determination by using fault slip and fluid inclusions planes data. J. Geophys. Res. 100 (B3), 3895–3904.
Lespinasse, M., Pêcher, A., 1986a. Microfracturing and regional stress field: a study of the preferred orientations of fluid-inclusion planes in a granite from the Massif Central, France. J. Struct. Geol. 8 (2), 169–180.
Lloyd, G.E., Knipe, R.J., 1992. Deformation mechanisms accommodating faulting of quartzite under upper crustal conditions. J. Struct. Geol. 14, 127–143.
Leroux, H., Reimold, W.U., Doukhan, J.C., 1994. A TEM investigation of shock metamorphism in quartz from the Vredefort dome, South Africa. Tectonophysics 230 (3), 223–239.
Mancktelow, N.S., Pennacchioni, G., 2013. Late magmatic healed fractures in granitoids and their influence on subsequent solid-state deformation. J. Struct. Geol. http://dx.doi.org/10.1016/j.jsg.2013.09.006.
Martin, P., Bergerat, F., 1996. Palaeo-stress inferred from macro- and microfractures in Balazuc-1 borehole (GPF programme). Contribution to the tectonic evolution of the Cevennes border of the SE basin of France. Mar. Petrol. Geol. 13, 671–684.
McLaren, A.C., Hobbs, B.E., 1972. Transmission electron microscope investigation of some naturally deformed quartzites. Geophys. Monogr. Ser. 16, 55–66.
Mitchell, T.M., Faulkner, D.R., 2009. The nature and origin of off-fault damage surrounding strike-slip fault zones with a wide range of displacements: a field study from the Atacama fault system, northern Chile. J. Struct. Geol. 31 (8), 802–816.
Mitchell, T.M., Faulkner, D.R., 2012. Toward quantifying the matrix permeability of fault damage zones in low porosity rocks. Earth Planet. Sci. Lett. 339–340, 24–31.
Mitra, S., 1987. Regional variations in deformation mechanisms and structural styles in the central Appalachian orogenic belt. Geol. Soc. Am. Bull. 98, 569–590.
Mizoguchi, K., Ueta, K., 2013. Microfractures within the fault damage zone record the history of fault activity. Geophys. Res. Lett. 40 (8), 2023–2027 http://dx.doi.org/10.1002/grl.50469.
Nadan, B.J., Engelder, T., 2009. Microcracks in New England granitoids: a record of thermoelastic relaxation during exhumation of intracontinental crust. Geol. Soc. Am. Bull. 121, 80–99.
Narahara, D.K., Wiltschko, D., 1986. Deformation in the hinge region of a chevron fold, Valley and Ridge province, central Pennsylvania. J. Struct. Geol. 8, 157–168.
Nur, A., Simmons, G., 1970. The origin of small cracks in igneous rocks. Int. J. Rock Mech. Mining Sci. 7, 307–314.
Onasch, C.M., 1990. Microfractures and their role in deformation of quartz arenite from the central Appalachian foreland. J. Struct. Geol. 12, 883–894.
Onasch, C.M., Dunne, W.M., Cook, J.E., O'Kane, A., 2009. The effect of fluid composition on the behavior of well cemented, quartz-rich sandstone during faulting. J. Struct. Geol. 31 (9), 960–971.

Onasch, C.M., Vennemann, T.W., 1995. Disequilibrium partitioning of oxygen isotopes associated with sector zoning in quartz. Geology 23 (12), 1103–1106.
Passchier, C.W., Trouw, R.J., 2005. Microtectonics. Springer Verlag, p. 322.
Plumb, R.A., Engelder, T., Yale, D., 1984. Near-surface in situ stress 3. Correlation with microcrack fabric within New Hampshire granites. J. Geophys. Res. 89, 9350–9364.
Power, W.L., Tullis, T.E., Brown, S.R., Boinott, G.N., Scholz, C.H., 1987. Roughness of natural fault surfaces. Geophys. Res. Lett. 14, 29–32.
Price, N.J., 1966. Fault and Joint Development in Brittle and Semi-brittle Rock. Pergamon, Oxford, p. 176.
Rempe, M., Mitchell, T., Renner, J., Nippress, S., Ben-Zion, Y., Rockwell, T., 2013. Damage and seismic velocity structure of pulverized rocks near the San Andreas Fault. J. Geophys. Res. 118, 2813–2831.
Ren, X., Kowallis, B.J., Best, M.G., 1989. Paleostress history of the Basin and Range province in western Utah and eastern Nevada from healed microcrack orientations in granites. Geology 17, 487–490.
Riley, N.A., 1947. Structural petrology of the Baraboo Quartzite. J. Geol. 55/6, 453–475.
Savage, H.M., Brodsky, E.E., 2011. Collateral damage: evolution with displacement of fracture distribution and secondary fault strands in fault damage zones. J. Geophys. Res. 116, B03405.
Segall, P., Pollard, D.D., 1980. Mechanics of discontinuous faults. J. Geophys. Res. 85 (B8), 4337–4350.
Shipton, Z.K., Cowie, P.A., 2001. Damage zone and slip-surface evolution over μm to km scales in high-porosity Navajo sandstone, Utah. J. Struct. Geol. 23 (12), 1825–1844.
Suzuki, T., 2012. Understanding of dynamic earthquake slip behavior using damage as a tensor variable: microcrack distribution, orientation, and mode and secondary faulting. J. Geophys. Res. 117, B05309.
Tarr, R.S., 1891. The phenomenon of rifting in granite. Am. J. Sci. (Third Series) CXLI, 267–272.
Vermilye, J.M., Scholz, C.H., 1998. The process zone: a microstructural view of fault growth. J. Struct. Geol. 103 (B6), 12,223–12,237.
Vollbrecht, A., Rust, S., Weber, K., 1991. Development of microcracks in granites during cooling and uplift: examples from the Variscan basement in NE Bavaria, Germany. J. Struct. Geol. 13, 787–799.
Vollbrecht, A., Stipp, M., Olesen, N.O., 1999. Crystallographic orientation of microcracks in quartz and inferred deformation processes: a study of gneisses from the German Continental Deep Drilling Project (KTB). Tectonophysics 303, 279–297.

Microfractures: fluids and diagenesis

Anderson, A.J., Bodnar, R.J., 1993. An adaptation of the spindle stage for geometric analysis of fluid inclusions. Am. Mineral. 78, 657–664.
Apaydin, O.G., Ozkan, E., Raghavan, R., 2012. Effect of discontinuous microfractures on ultratight matrix permeability of a dual-porosity medium. SPE Reserv. Eval. Eng. 15, 473–485.
Bai, T., Pollard, D.D., Gao, H., 2000. Explanation for fracture spacing in layered material. Nature 403 (6771), 753–756.
Batzle, M.L., Simmons, G., 1976. Microfractures in rocks from two geothermal areas. Earth Planet. Sci. Lett. 30/1, 71–93.
Becker, S.P., Eichhubl, P., Laubach, S.E., Reed, R.M., Lander, R.H., Bodnar, R.J., 2010. A 48 m.y. history of fracture opening, temperature, and fluid pressure: Cretaceous Travis Peak Formation, East Texas basin. Geol. Soc. Am. Bull. 122, 1081–1093.
Boiron, M.C., Essarraj, S., Sellier, E., Cathelineau, M., Lespinasse, M., Poty, B., 1992. Identification of fluid inclusions in relation to their host microstructural domains in quartz by cathodoluminescence. Geochim. Cosmochim. Acta 56 (1), 175–185.
Boullier, A.-M., 1999. Fluid inclusions: tectonic indicators. J. Struct. Geol. 21 (8), 1229–1235.
Boullier, A.-M., Robert, F., 1992. Textures and orientation of fluid inclusion planes in gold-quartz vein networks, Val d'Or, Abitibi, Quebec, Canada. J. Struct. Geol. 14, 161–179.
Brantley, S.L., 1990. The effect of fluid chemistry on quartz microcrack lifetimes. Earth Planet. Sci. Lett. 113, 145–156.
Brantley, S.L., Evans, B., Hickman, S.H., Crerar, D.A., 1990. Healing of microcracks in quartz: implications for fluid flow. Geology 18, 136–139.
Burley, S.D., Mullis, J., Matter, A., 1989. Timing diagenesis in the Tartan reservoir (UK North Sea): constraints from combined cathodoluminescence and fluid inclusion studies. Mar. Petrol. Geol. 6, 98–120.
Capuano, R.M., 1993. Evidence of fluid flow in microfractures in geopressured shales. AAPG Bull. 77 (8), 1303–1314.
Cathelineau, M., Lespinasse, M., Bastoul, A.M., Bernard, C., Leroy, J., 1990. Fluid migration during contact metamorphism: the use of oriented fluid inclusion trails for a time/space reconstruction. Mineral. Mag. 54 (2), 169–172.
Crawford, M.L., 1992. Fluid inclusions – what can we learn? Earth Sci. Rev. 32, 137–139.
Davies, G.R., Smith, L.B., 2006. Structurally controlled hydrothermal dolomite reservoir facies: an overview. AAPG Bull. 90 (11), 1641–1690.
Davy, P., Le Groc, R., Darcel, C., Bour, O., de Dreuzy, J.R., Munier, R., 2010. A likely universal model of fracture scaling and its consequence for crustal hydromechanics. J. Geophys. Res. 115, B10411, http://dx.doi.org/10.1029/2009JB007043.
Dickenson, W.W., Milliken, K.L., 1995. The diagenetic role of brittle deformation in compaction and pressure solution, Etjo sandstone, Namibia. J. Geol. 103/3, 339–347.
Eichhubl, P., Hooker, J.N., Laubach, S.E., 2010. Pure and shear-enhanced compaction bands in Aztec Sandstone. J. Struct. Geol. 32 (12), 1873–1886 http://dx.doi.org/10.1016/j.jsg.2010.02.004.
Ellis, M.A., Laubach, S.E., Eichhubl, P., Olson, J.E., Hargrove, P., 2012. Fracture development and diagenesis of Torridon Group Applecross Formation, near An Teallach, NW Scotland: millennia of brittle deformation resilience? J. Geol. Soc. Lond. 169, 297–310.
Engvik, A.K., Bertram, A., Kalthoff, J.F., Stöckhert, B., Austrheim, H., Elvevold, S., 2005. Magma-driven hydraulic fracturing and infiltration of fluids into the damaged host rock, an example from Dronning Maud Land, Antarctica. J. Struct. Geol. 27 (5), 839–854.
Engvik, L., Stöckhert, B., Engvik, A.K., 2009. Fluid infiltration, heat transport, and healing of microcracks in the damage zone of magmatic veins: numerical modeling. J. Geophys. Res. 114 (B5), B05203.
Evans, M.A., 1995. Fluid inclusions in veins from the Middle Devonian shales: a record of deformation conditions and fluid evolution in the Appalachian Plateau. Geol. Soc. Am. Bull. 107, 327–339.
Fall, A., Eichhubl, P., Cumella, S.P., Bodnar, R.J., Laubach, S.E., Becker, S.P., 2012. Testing the basin-centered gas accumulation model using fluid inclusion observations: Southern Piceance Basin, Colorado. AAPG Bull. 96 (12), 2297–2318 http://dx.doi.org/10.1306/05171211149.
Fischer, M.P., Higuera-Diaz, I.C., Evans, M.A., Perry, E.C., Lefticariu, L., 2009. Fracture-controlled paleohydrology in a map-scale detachment fold: insights from the analysis of fluid inclusions in calcite and quartz veins. J. Struct. Geol. 31, 1490–1510.
Fisher, Q.J., Casey, M., Harris, S.D., Knipe, R.J., 2003. Fluid-flow properties in sandstone: the importance of temperature history. Geology 3/11, 965–968. http://dx.doi.org/10.1130/G19823.1.
Gale, J.F.W., 2002. Specifying lengths of horizontal wells in fractured reservoirs. SPE Reserv. Eval. Eng. 5 (3), 266–272.
Gale, J.F.W., Laubach, S.E., Marrett, R.A., Olson, J.E., Holder, J., Reed, R.M., 2004. Predicting and characterizing fractures in dolostone reservoirs: using the link between diagenesis and fracturing. The geometry and petrogenesis of dolomite hydrocarbon reservoirs. In: Geological Society of London, Special Publication, vol. 235, pp. 177–192.
Gale, J.F.W., Reed, R.M., Holder, J., 2007. Natural fractures in the Barnett Shale and their importance for hydraulic fracture treatments. AAPG Bull. 91, 603–622.
Gale, J.F.W., Lander, R.H., Reed, R.M., Laubach, S.E., 2010. Modeling fracture porosity evolution in dolostone. J. Struct. Geol. 32 (9), 1201–1211 http://dx.doi.org/10.1016/j.jsg.2009.04.018.
Gale, J.F.W., Laubach, S.E., Olson, J.E., Eichhubl, P., Fall, A., 2014. Natural fractures in shale: a review and new observations. AAPG Bull. (in press).
Goldstein, R.H., Reynolds, T.J., 1994. Systematics of fluid inclusions in diagenetic minerals. In: SEPM (Society for Sedimentary Geology) Short Course, vol. 31, p. 199.
Guerriero, V., Iannace, A., Mazzoli, S., Parente, M., Vitale, S., Giorgioni, M., 2010. Quantifying uncertainties in multi-scale studies of fractured reservoir analogues: implemented statistical analysis of scan line data from carbonate rocks. J. Struct. Geol. 32, 1271–1278.
Hay, S.J., Hall, J., Simmons, G., Russell, M.J., 1988. Sealed microcracks in the Lewisian of NW Scotland: a record of 2 billion years of fluid circulation. J. Geol. Soc. Lond. 145, 819–830.
Hilgers, C., Kirschner, D.L., Breton, J.-P., Urai, J.L., 2006. Fracture sealing and fluid overpressures in limestones of the Jabal Akhdar dome, Oman mountains. Geofluids 6, 168–184.
Hooker, J.N., Laubach, S.E., 2007. The geologic history of quartz grains, as revealed by color SEM-CL. Gulf Coast Assoc. Geol. Soc. Trans. 57, 375–386.
Hu, M.S., Evans, A.G., 1989. The cracking and decohesion of thin-films on ductile substrates. Acta Metall. 37 (3), 917–925.
Kranz, R.L., Frankel, A.D., Engelder, T., Scholz, C.H., 1979. The permeability of whole and jointed Barre Granite. Int. J. Rock Mech. Min. Sci. Abstr. 16, 225–234.
Kruhl, J.H., Wirth, R., Morales, L.F.G., 2013. Quartz grain boundaries as fluid pathways in metamorphic rocks. J. Geophys. Res. 118, 1–11.
Kupecz, J.A., Land, L.S., 1991. Late diagenetic dolomitization of the Lower Ellenburger group, West Texas. J. Sediment. Petrol. 61 (4), 551–574.
Lander, R.H., Larese, R.E., Bonnell, L.M., 2008. Toward more accurate quartz cement models – the importance of euhedral vs. non-euhedral growth rates. AAPG Bull. 92, 1537–1564.
Lander, R.H., Laubach, S.E., 2014. Insights into rates of fracture growth and sealing from a model of quartz cementation in fractured sandstones. GSA Bull..
Lash, G.G., Engelder, T., 2005. An analysis of horizontal microcracking during catagenesis: example from the Catskill delta complex. AAPG Bull. 89, 1433–1449.
Laubach, S.E., 1988a. Fractures generated during folding of the Palmerton Sandstone, Eastern Pennsylvania. J. Geol. 96, 495–503.
Laubach, S.E., 1988b. Subsurface fractures and their relationship to stress history in East Texas Basin sandstone. Tectonophysics 156, 37–49.
Laubach, S.E., 1989. Paleostress directions from the preferred orientation of closed microfractures (fluid-inclusion planes) in sandstone, East Texas basin, U.S.A. J. Struct. Geol. 11/5, 603–611.
Laubach, S.E., 1997. A method to detect natural fracture strike in sandstones. AAPG Bull. 81 (4), 604–623.

Laubach, S.E., 2003. Practical approaches to identifying sealed and open fractures. AAPG Bull. 87 (4), 561–579.
Laubach, S.E., Reed, R.M., Olson, J.E., Lander, R.H., Bonnell, L.M., 2004a. Coevolution of crack-seal texture and fracture porosity in sedimentary rocks: cathodoluminescence observations of regional fractures. J. Struct. Geol. 26 (5), 967–982.
Laubach, S.E., Ward, M.E., 2006. Diagenesis in porosity evolution of opening-mode fractures, Middle Triassic to Lower Jurassic La Boca Formation, NE Mexico. Tectonophysics 419 (1–4), 75–97.
Lemmlein, G.C., Kliya, M.O., 1960. Distinctive features of the healing of a crack in a crystal under conditions of declining temperature. Int. Geol. Rev. 2, 125–128.
Lespinasse, M., 1999. Are fluid inclusion planes useful in structural geology? J. Struct. Geol. 21 (8), 1237–1243.
Lespinasse, M., Cathelineau, M., 1990. Fluid percolations in a fault zone: a study of fluid inclusion planes in the St Sylvestre granite, northwest Massif Central, France. Tectonophysics 184 (2), 173–187.
Lespinasse, M., Désindes, L., Fratczak, P., Petrov, V., 2005. Microfissural mapping of natural cracks in rocks: implications for fluid transfers quantification in the crust. Chem. Geol. 223 (1), 170–178.
Marquez, X.M., Mountjoy, E.W., 1996. Microfractures due to overpressures caused by thermal cracking in well-sealed Devonian reservoirs, deep Alberta basin, Canada. AAPG Bull. 80 (4), 570–588.
Meere, P.A., 1995. High and low density fluids in a quartz vein from the Irish Variscides. J. Struct. Geol. 17 (3), 435–446.
Milliken, K.L., 1994. The widespread occurrence of healed microfractures in siliciclastic rocks: evidence from scanned cathodoluminescence imaging. In: Nelson, P.P., Laubach, S.E. (Eds.), Rock Mechanics: Models and Measurements, Challenges from Industry, 1st North American Rock Mechanics Symposium. A.A. Balkema, Rotterdam, pp. 825–832.
Milliken, K.L., Laubach, S.E., 2000. Brittle deformation in sandstone diagenesis as revealed by scanned cathodoluminescence imaging with application to characterization of fractured reservoirs. In: Pagel, M., Barbin, V., Blanc, P., Ohnenstetter, D. (Eds.), Cathodoluminescence in Geosciences. Springer Verlag, New York, pp. 225–243 (Chapter 9).
Milliken, K.L., Reed, R.M., Laubach, S.E., 2005. Quantifying compaction and cementation within deformation bands in porous sandstones. In: Sorkhabi, R., Tsuji, Y. (Eds.), Faults, Fluid Flow and Petroleum Traps, AAPG Memoir, vol. 85, pp. 237–249.
Montanez, I.P., Read, J.F., 1992. Fluid-rock interaction history during stabilization of early dolomites, upper Knox Group (Lower Ordovician), US Appalachians. J. Sediment. Res. 62 (5), 753–778.
Mork, M.B.E., Moen, K., 2007. Compaction microstructures in quartz grains and quartz cement in deeply buried reservoir sandstones using combined petrography and EBSD analysis. J. Struct. Geol. 29 (11), 1843–1854.
Nelson, R.A., 1985. Geologic Analysis of Naturally Fractured Reservoirs. Gulf Publishing, Houston, p. 320.
Olson, J.E., Laubach, S.E., Lander, R.H., 2009. Natural fracture characterization in tight gas sandstones: integrating mechanics and diagenesis. AAPG Bull. 93, 1535–1549.
Pagel, M., Barbin, V., Blanc, P., Ohnenstetter (Eds.), 2000. Cathodoluminescence in Geosciences. Springer-Verlag,, New York.
Pêcher, A., Lespinasse, M., Leroy, J., 1985. Relations between fluid inclusion trails and regional stress field: a tool for fluid chronology – an example of an intragranitic uranium ore deposit (northwest Massif Central, France). Lithos 18, 229–237.
Roberts, J.C., 1965. Quartz microfracturing in the north crop of the South Wales Coalfield. Geol. Mag. 102, 59–72.
Roedder, E., 1984. Fluid inclusions. In: Ribbe, P.H. (Ed.), Reviews in Mineralogy, vol. 12. Mineralogical Society of America, Washington, D.C, p. 644.
Sibley, D.F., Blatt, H., 1976. Intergranular pressure solution and cementation of the Tuscarora orthoquartzite. J. Sediment. Res. 46, 881–896.
Sipple, R.F., 1968. Sandstone petrology, evidence from luminescence petrography. J. Sediment. Petrol. 38, 530–554.
Smith, D.L., Evans, B., 1984. Diffusional crack healing in quartz. J. Geophys. Res. 89, 4125–4135.
Sprunt, E.S., Nur, A., 1979. Microcracking and healing in granites: new evidence from cathodoluminescence. Science 205, 495–497.
Tuttle, O.F., 1949. Structural petrology of planes of liquid inclusions. J. Geol. 57, 331–356.
Travé, A., Labaume, P., Vergés, J., 2007. Fluid systems in foreland fold-and-thrust belts: an overview from the southern Pyrenees. In: Lacombe, O., Roure, F., Lavé, J., Vergés, J. (Eds.), Thrust Belts and Foreland Basins. Springer, Berlin, pp. 93–115.
Walderhaug, O., 1994. Precipitation rates for quartz cement in sandstones determined by fluid-inclusion microthermometry and temperature-history modeling. J. Sediment. Res. A64 (2), 324–333.
Walsh, J.B., Brace, W.F., 1984. The effect of pressure on porosity and the transport properties of rock. J. Geophys. Res. 89 (B11), 9425–9431.
Wise, D.U., 1964. Microjointing in basement, middle Rocky Mountains of Montana and Wyoming. Geol. Soc. Am. Bull. 75, 287–306.

Microfractures: geophysical properties

Crampin, S., 1987. Geological and industrial applications of extensive-dilatancy anisotropy. Nature 328, 491–496.
Crampin, S., 1994. The fracture criticality of crustal rocks. Geophys. J. Int. 118 (2), 428–438.
Hall, J., 1987. Physical properties of Lewisian rocks: implications for deep crustal structure. In: Geological Society of London, Special Publication, vol. 27, pp. 185–192.
Marrett, R., Laubach, S.E., Olson, J.E., 2007. Anisotropy and beyond: geologic perspectives on geophysical prospecting for natural fractures. Leading Edge 26/9, 1106–1111.
Sayers, C.M., Kachanov, M., 1995. Microcrack-induced elastic wave anisotropy of brittle rocks. J. Geophys. Res. 100 (B3), 4149–4156 http://dx.doi.org/10.1029/94JB03134.

Microfractures: joints, veins, and lamellae

Baecher, G.B., Lanney, N.A., 1978. Trace length biases in joint surveys. In: 19th U.S. Symposium on Rock Mechanics. University of Nevada, Reno, pp. 56–65.
Boggs Jr., S., Krinsley, D., 2006. Application of Cathodoluminescence Imaging to the Study of Sedimentary Rocks. Cambridge University Press, Cambridge, p. 165.
Böhm, A., 1883. Über Gesteine des Wechsels. Tschermaks Mineral. Petrogr. Mitteil. 5, 197–214.
Christie, J.M., Raleigh, C.B., 1959. The origin of deformation lamellae in quartz. Am. J. Sci. 257, 385–407.
Dale, T.N., 1908. The chief commercial granites of Massachusetts, New Hampshire, and Rhode Island. U.S. Geol. Surv. Bull. 354, 228.
Dale, T.N., 1923. The commercial granites of New England. U.S. Geol. Surv. Bull. 738, 488.
Delaney, P.T., Pollard, D.D., Ziony, J.I., McKee, E.H., 1986. Field relations between dikes and joints – emplacement processes and paleostress analysis. J. Geophys. Res. – Solid Earth 91, 4920–4938.
Drury, M.R., 1993. Deformation lamellae in metals and minerals. In: Boland, J.N., Fitzgerald, J.D. (Eds.), Defects and Processes in the Solid State: Geoscience Applications: McLaren Volume. Elsevier, Amsterdam, The Netherlands, pp. 195–212.
Fleischmann, K.H., 1990. Rift and grain in two granites of the White Mountain magma series. J. Geophys. Res. 95, 21463–21474.
Gillespie, P.A., Walsh, J.J., Watterson, J., Bonson, C.G., Manzocchi, T., 2001. Scaling relationships of joint and vein arrays from The Burren, Co. Clare, Ireland. J. Struct. Geol. 23, 183–201.
Gomez, L.A., Laubach, S.E., 2006. Rapid digital quantification of microfracture populations. J. Struct. Geol. 28, 408–420.
Groshong, R.H., 1988. Low-temperature deformation mechanisms and their interpretation. Geol. Soc. Am. Bull. 100, 1329–1360.
Harper, M.L., 1966. Joints and microfractures in Glenwood Canyon, Colorado. Mountain Geol. 3 (4), 185–192.
Holzhausen, G.R., 1977. Sheet Structure in Rock and Some Related Problems in Rock Mechanics. Stanford University. Unpublished Ph.D. dissertation.
Ingerson, E., Tuttle, O.F., 1948. Relations of lamellae and crystallography of quartz and fabric directions in some deformed rocks. Am. Geophys. Union Trans. 26, 95–105.
Laubach, S.E., Marrett, R., Olson, J., Scott, A.R., 1998. Characteristics and origins of coal cleat: a review. Int. J. Coal Geol. 35, 175–207.
Lyell, C., Deshayes, G.P., 1830. Principles of Geology: Being An Attempt to Explain the Former Changes of the Earth's Surface, by Reference to Causes Now in Operation, vol. 1. John Murray, London.
Ortega, O.O., Marrett, R., 2000. Prediction of macrofracture properties using microfracture information, Mesaverde Group sandstones, San Juan Basin, New Mexico. J Struct Geol 22, 571–588.
Pollard, D.D., Aydin, A., 1988. Progress in understanding jointing over the past century. Geol. Soc. Am. Bull. 100, 1181–1204.
Tuttle, O.F., 1945. Relations of lamellae and crystallography of quartz and fabric directions in some deformed rocks. Am. Geophys. Union Trans. XXVI, 95–105.

Please cite this article in press as: Anders, M.H., et al., Microfractures: A review, Journal of Structural Geology (2014), http://dx.doi.org/10.1016/j.jsg.2014.05.011